

TECHNISCHE UNIVERSITÄT MÜNCHEN

**Deutsches Herzzentrum München und
1. Medizinische Klinik, Klinikum rechts der Isar,
(Direktor: Univ.-Prof. Dr. A. Schömig)**

Genetic disruption of the kindlin-3/ β 1-integrin interaction results in defective β 1-integrin dependent platelet adhesion and granula secretion

Tobias Petzold

Vollständiger Abdruck der von der Fakultät für Medizin der Technischen Universität München zur Erlangung des akademischen Grades eines

Doktors der Medizin

genehmigten Dissertation.

Vorsitzender: Univ.-Prof. Dr. E. J. Rummeny

Prüfer der Dissertation:

1. Univ.-Prof. Dr. St. Massberg
2. Priv.-Doz. Dr. I. V. Deisenhofer
3. Univ.-Prof. Dr. J. G. Duyster (schriftliche Beurteilung)
3. Univ.-Prof. Dr. St. Engelhardt (mündliche Prüfung)

Die Dissertation wurde am 12.09.2011 an der Technischen Universität München eingereicht und durch die Fakultät für Medizin am 26.09.2012 angenommen.

Table of contents	page
<u>Abbreviations</u>	IV
<u>Figures</u>	VI
<u>1. Introduction</u>	1
1.1 Platelets in arterial thrombosis	1
1.2 Integrins	2
1.2.1 Integrin function	3
1.2.2 Platelet integrins	4
1.3 Role of platelet β1 integrins	5
1.4 Integrin activation and the role of talin and kindlin	6
1.5 From platelet activation to integrin activation	8
1.6 Clinical relevance of kindlin-3 in leucocyte adhesion deficiency type III	9
1.7 Clinical relevance of α2β1 integrins in arterial thrombosis	10
<u>2. Aims of the study</u>	12
<u>3. Materials and Methods</u>	13
3.1 Animal work	13
3.1.1 Genetics	13
3.1.2 Genotyping of animals	14
3.1.3 Generation of bone marrow chimeras	15
3.1.4 Carotid ligation model	16
3.1.5 Bleeding time assay	16
3.2 Protein work	16

3.2.1 Bacterial transformation and bacterial culture	16
3.2.2 Integrin tail peptide production	17
3.2.3 Protein purification	18
3.2.4 Protein concentration determination by Bradford method	18
3.2.5 UV spectroscopy to determine protein concentration	19
3.2.6 Pulldown assays	19
3.2.7 Immunoblotting	20
3.2.7.1 Stripping of western blot	21
3.2.7.2 Coomassie staining	21
3.2.8 Integrin phosphorylation analysis	22
3.3 Platelet work	22
3.3.1 Platelet isolation	22
3.3.2 Flow cytometry	22
3.3.3 Platelet spreading	23
3.3.4 $\beta 1$ integrin staining	24
3.3.5 Aggregation assay	24
3.3.6 Fibrinogen secretion assay	25
3.3.7 Evaluation of ATP release from dense granula	25
3.4 Statistical analysis	25
<u>4. Results</u>	<u>26</u>
4.1 Integrin tail-peptide production and pulldown experiments	26
4.2 Experimental design and generation of $\beta 1^{TAA/fl}$ MxCre and $\beta 1^{Hpm/fl}$ MxCre mice	29

4.3 Platelet characterization	30
4.4 Integrin activation assays	32
4.5 Platelet spreading	34
4.6 Tailbleeding assay	38
4.7 Carotid ligation assay	40
4.8 Aggregation assays	41
4.9 Dense granula and α-granula secretion	44
4.10 Integrin tail phosphorylation	46
<u>5. Discussion</u>	<u>48</u>
5.1 $\beta 1^{\text{TTAA}}$ integrins	48
5.1.1 $\beta 1^{\text{TTAA}}$ integrin outside-in signaling	48
5.1.2 Integrin tail binding partner	49
5.1.3 Threonine phosphorylation of the integrin tail	50
5.1.4 $\beta 1^{\text{TTAA}}$ expression level	51
5.2 $\beta 1$ integrins in arterial thrombosis	51
5.2.1 Bone marrow chimera	52
5.2.2 Carotid ligation assay and occlusive thrombus formation	52
5.2.3 Aggregation and secretion	54
<u>6. Summary</u>	<u>56</u>
<u>7. Zusammenfassung</u>	<u>57</u>
<u>References</u>	<u>58</u>
<u>Curriculum vitae</u>	<u>63</u>

Abbreviations

ACD	Blood coagulation buffer based on citrate-ions
ADP	Adenosindiphosphat
C 807/ G 873	DNA base pair cytosine 807, guanine 873
CD	Cluster of diffentiation
CRP	Collagen related peptide
CVX	Convulxin
DAG	Diacylglycerol
DCF	Dichloroflourescein
DIC	Differential interference contrast
DNA	Desoxy- ribonucleic acid
dNTP	Desoxynucleoside triphosphate
ECM	extracellular matrix
EDTA	Ethylenediaminetetraacetic acid
FAK	Focal adhesion kinase
FcR γ	Fc Receptor- γ
FERM	Four- point-one, Ezrin, Radixin, Moesin Domain
FITC	Flourescein isothiocyanate
GAPDH	Glycerinaldehyd 3- phosphat- dehydrogenase
GEF	Guanodin nucleotid-exchange-factors
GFOGER	Amino acid sequence: Glycin-Phenylalanine-Pyrrolysine- Glycine- Glutamic acid- Arginine
GPIb α	Glycoprotein Iba
GPIX	Glycoprotein IX
GPV/	Glycoprotein V
GPVI	Glycoprotein VI
GTP	Guanosin tri phosphate
HCL	Hydrogen chloride
HIS	Histidine
HPLC	High pressure liquid chromatography
Hpm	Platelets , genotype: $\beta 1^{Hpm/-}$ integrin
HRP	Horse radish peroxidase
HT	$\beta 1^{-/+}$ Heterozygous platelets
HT	Platelets , genotype: $\beta 1^{+/-}$ integrin
I- domain	Inserted domain
ICAM-1	Inter- cellular adhesion molecule 1
Ig	Imunoglobulin
ILK	Integrin linked kinase
IP3	Inositol- triphosphate
IPTG	Isopropyl-beta-D-thiogalactopyranoside
ITAM	Immunoreceptor tyrosine based activation motif
KO	Knock out platelets $\beta 1^{-/-}$ integrin
LAD III/ 3	Leucocyte adhesion deficiency type III / 3
LB medium	Lysogeny broth
MAPK	Mitogen activated protein kinase
MIDAS	Metal ion dependent adhesion site
MxCre	Mx1- promoter driven Cre- Recombinase Gene
NF κ B	Nuclear factor κ B
NMD	Nonsense mediated RNA decay

NPxY	Amino acid sequence: Asparagine- Prolin- X – Tyrosine
NTA	Nitrinoltriacetic acid
PBS	Phosphate buffered saline
PCR	Polymerase chain reaction
PD Buffer	Pulldown buffer
PDVF	Polyvinylidene flouride
PE	Phycoerythin
petB16	Expression plasmid for bacterial transfection
PFA	Paraformaldehyde
PKC	Protein kinase C
PLC2 γ	Phospholipase C 2 γ
POLY I:C	POLY I(Iosine):C(Cytidine)
PTB	Phosphotyrosine- binding domain
Rap 1	Ras- related protein
RIAM	Rap1–GTP-interacting adapter molecule
RNA	Ribonucleic acid
RPM	Rounds per minute
RT	Room temperature
SDS	Sodium dodecyl sulfate
SEM	Standard error mean
SH2 domain	Src homology domain 2
SILAC	Stable isotope labeling with amino acids in cell culture
SOCE	Store-operated Ca ²⁺ entry
T 807 / A 873	DNA base pair Thymine 807, Adenine 873
TBST	Tris buffered salins with TWEEN
TEMED	Tetramethylethylendiamin
TFA	Tri-flour-acid
TIRF	Total interference reflection fluorecence
Tris	Tris(hydroxymethyl)aminomethane
TT/AA	β 1 ^{TTAA/-} mutated platelets
TT/AA	Platelets carrying a β 1 ^{TTAA/-} integrin
U/ml	Units/milliliter
U46619	Thromboxane- A
UV	Ultra violet
VCAM-1	Vascular cell adhesion molecule 1
vWF	von Willebrand factor
WT	Platelets genotype β 1 ^{+/+} integrin (wild type)
Xg	Multiple of g force
α IIb β IIIa	α 2b β 3a integrin
α v β III	α v β 3 integrin

Figures

Supplementary Figure 1: Platelet adhesion and aggregation on the ECM (from David Varga-Szabo et al. 2008(7))	2
Supplementary figure 2: Integrin inside-out signalling (activation)	8
Figure 1: Amino-acid sequences of $\beta 1$ integrin tail and bacterial expressed peptide sequence	27
Figure 2: Pulldown experiment	28
Figure 3: Experimental design	29
Figure 4: Characterization of platelets	31
Figure 5: $\beta 1$ integrin activation is reduced in $\beta 1^{\text{TAAV-}}$ platelet	33
Figure 6: $\beta 1$ integrins form an adhesive ring at the outer circumference of spread platelets	35
Figure 7: Spreading of thrombin stimulated platelets	37
Figure 8: $\beta 1^{\text{TAAV-}}$ platelets show a defect outside-in signaling and FAK phosphorylation which can be rescued by addition of manganese	38
Figure 9: $\beta 1^{-/-}$ and $\beta 1^{\text{TAAV-}}$ mice show prolonged bleeding times	39
Figure 10: Single platelet adhesion analyzed in a carotid ligation model	40
Figure 11: $\beta 1$ integrins are required for fibrillar collagen induced aggregation in vitro	42
Figure 12: Presence of fibrinogen or Mn^{2+} can rescue aggregation defect in $\beta 1^{\text{TAAV-}}$ platelets	43
Figure 13: $\beta 1$ integrins are required for fibrinogen secretion after collagen stimulation	45
Figure 14: Dense granula secretion upon fibrillar collagen stimulation depends	

on β 1Integrin

46

Figure 15: β 1 integrins are phosphorylated in vivo, potentially by PKC family

kinases

47

1. Introduction

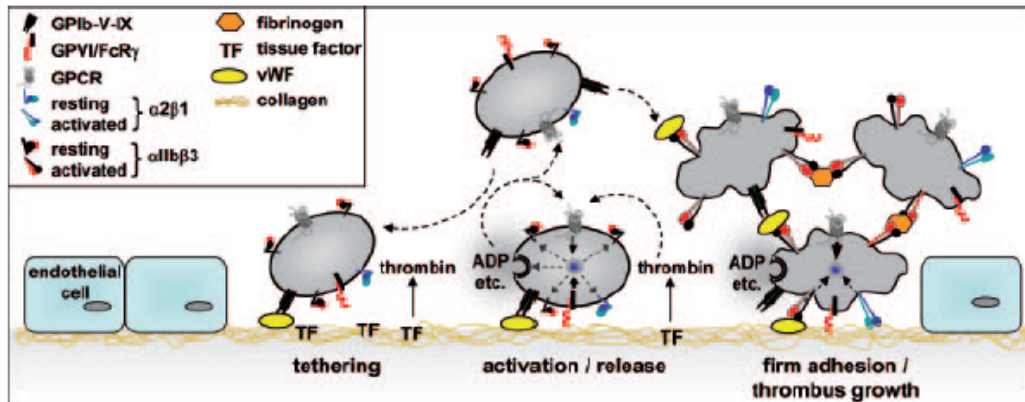
1.1 Platelets in arterial thrombosis

Platelets represent the major cellular components of the hemostatic system. They are constantly sheared off from transendothelial proplatelets, which are protrusions of bone marrow megakaryocytes. This process is referred to as thrombopoiesis (1). Once released into the blood, platelets patrol the vascular system in close proximity to the vessel wall in search for vascular injuries. When they get in contact with vessel wall lesions they become rapidly activated, which leads to platelet adhesion, aggregation and finally wound closure.

The molecular mechanisms that initiate primary hemostasis are well understood (2). Subendothelial lesions accompany with the exposure of various matrix components, which are recognized and bound by different platelet receptors. Platelets exhibit the GPIb-GPV-GPIX complex (around 25000 copies/cell) on their surface (3). In vivo and in vitro analyses have shown that under high shear conditions initial platelet adhesion to sites of vascular injuries or an activated endothelium is mediated by the interaction between GPIb(α) on platelets and vWF, which is either bound to extracellular matrix (ECM) collagen or exposed by the activated endothelium (4). The interaction of GPIb with an activated endothelium was shown to promote leukocyte recruitment and atherosclerotic plaque formation in Apoprotein- E deficient mice (4).

However, during thrombus formation GPIb interactions are only transient and result in the deceleration and rolling of platelets, enabling other surface receptors to bind to the extracellular exposed matrices including collagen. Collagen belongs to the most thrombogenic matrix components of subendothelial lesions and is bound by GPVI and $\alpha 2\beta 1$ integrin surface receptors. GPVI forms a non-covalently bound complex with FcR γ (5). Once the receptor is engaged to collagen it forms a GPVI homodimer which leads to tyrosine phosphorylation of the immunoreceptor tyrosine-based activation motif (ITAM) within the FcR γ by Src family kinases (6). GPVI signaling (9) triggers auto- and paracrine granula secretion and exposure of strong platelet activators such as Thromboxane- A₂, ADP as well as a variety of procoagulant molecules including vWF, Fibrinogen, integrin $\alpha 11\beta 3$ or P-selectine (7). Due to the release of these components, platelets contribute to a

prothrombotic and procoagulant environment at the lesion site (3). On the other hand, GPVI signals trigger the activation of surface receptors, such as $\alpha\text{IIb}\beta\text{3}$ and β1 integrins, which play fundamental roles in mediating platelet-matrix and platelet-platelet interactions (8) (*Supplementary Figure 1*).



Supplementary Figure 1: Platelet adhesion and aggregation on the ECM (from David Varga-Szabo et al. 2008(7)). The GPIb- vWF interaction mediates platelet tethering thereby enabling GPVI interaction with collagen. This triggers the shift of integrins to a high-affinity state and release of ADP and Thromboxane A2. In parallel, tissue factor (TF) locally triggers thrombin formation which also contributes to platelet activation.

1.2 Integrins

Integrins represent the largest family of adhesion receptors which are exclusively expressed in metazoans. Integrins resemble heterodimeric transmembrane molecules consisting of non-covalently bound α and β subunits (9). To date 18 β and 8 α subunits are known, which form 24 different heterodimers. Both integrin subunits have a large extracellular domain consisting of ≥ 1600 aminoacids, whereas the intracellular tails (except for β4 integrin) are relatively short with about 20- 50 aminoacids. The extracellular regions of integrin subunits consist of a stalk like amino acid chain attached via a bend “knee region” to a globular- head-domain, which facilitates a ligand recognition site. Some α -subunits (i.e. α1 , α2 , αL , and αX , αM) expose a so-called I domain (inserted domain), which harbors a metal ion dependent adhesion site (MIDAS) coordinating the binding of an Mg^{2+} ion. The β1 integrin head domain consists of a βA - domain that also contain

several MIDAS. Therefore ligand binding to integrins such as $\alpha 2\beta 1$ depends on extracellular ion concentrations and can be induced by extracellular addition of ions such as Mn^{2+} , irrespective of the intracellular activation mode (see below) (10).

1.2.1 Integrin function

Integrins connect the intracellular cytoskeleton with the extracellular matrix. They act as bidirectional signaling machines which transmit mechanical forces via the plasma membrane in both directions. They are involved in various cellular processes such as cell spreading, migration, tumor metastasis, adhesion and cell survival (9, 11). Integrin derived signals maintain cell survival of most cell types (except for hematopoietic derived cells), as depriving integrin-extracellular matrix interactions leads to programmed cell death referred as “Anoikis”, a mechanism which is bypassed in tumor cells (12). Most importantly, $\beta 1$ integrins are indispensable during embryonic development. $\beta 1$ integrin deficient mouse embryos develop normally until the blastocyst is formed. However already at this stage the inner cell mass fails to develop normally and dies due to a retarded growth shortly after the trophoblast had invaded the uterus (13).

The rising field of mechanotransduction addresses mechanisms by which physical stimuli are translated into a biological response on a molecular level. In this context, integrins were found to be major players with particular importance during the development of cardiovascular diseases (14-15). Atherosclerotic lesions develop preferentially at regions of so called turbulent flow within the vasculature. Turbulent flow patterns are found at the inner side of the aortic arch and at the outer side in carotid bifurcations. In these atheroprone regions, endothelial cell integrins are kept in an active state due to a continuously changing directionality of the blood flow and of locally exerted shear forces. Molecular studies found, that permanently activated integrins induce and maintain proinflammatory signaling pathways such as the activation of NF κ B, a transcription factor that binds to κ B response elements found in promoter regions of many inflammatory receptors such as ICAM-1 or VCAM-1 (16). The expression of these adhesion proteins leads to increased recruitment of inflammatory cells to the vessel wall, a key event in the development of arteriosclerosis. The importance for a differential $\beta 1$ integrin

signaling in this process was convincingly demonstrated in vitro by Orr et al. (17). Endothelial cells seeded on fibronectin, a substrate for $\alpha 5\beta 1$ integrin that accumulates at atheroprone regions within the vasculature, show an inflammatory activation state with sustained NF κ B activation once they are exposed to shear stress. In contrast, cells seeded on collagen (the main ECM component of healthy vasculature), which anchor via $\alpha 2\beta 1$ integrins, exhibit a silent, non-inflammatory phenotype under the same experimental settings. The authors suggested that atheroprotective behavior depends on the activation of p38–MAPK (17) downstream of $\alpha 2\beta 1$ integrins.

So far it remains difficult to delineate signaling events emerging from activated integrins. Integrin outside-in signaling arises as soon as a specific ligand is bound and a multifaceted complex signaling platform, referred to as the adhesome (18) is formed. The adhesome involves more than 150 proteins that arrange in different signaling platforms with a certain local and temporal resolution depending on the surrounding microenvironment and activation state of the integrin (19).

1.2.2 Platelet integrins

Platelets express a series of integrins namely $\alpha IIb\beta 3$, $\alpha v\beta 3$, $\alpha 2\beta 1$, $\alpha 5\beta 1$, and $\alpha 6\beta 1$, which have different ligand specificities. The $\alpha IIb\beta 3$ integrin (20) is the most abundant platelet integrin and binds to various ligands such as fibrinogen, vWF, and fibronectin. It is fundamental for platelet adhesion and aggregation and therefore represents the physiologically and therapeutically most relevant integrin. Clinical treatment with Abciximab, an integrin $\alpha IIb\beta 3$ inhibiting chimeric antibody, protects efficiently from arterial thrombosis, while increasing the risk of severe bleedings (21). Some patients suffering from Glanzmann thrombasthenia show mutations in $\beta 3$ or the αIIb integrin subunit that cause either reduced receptor expression or severe functional defects of the integrin. These patients usually reveal a broad spectrum from minor to extensive, life threatening bleedings already at young ages (22). Similar observation can be seen in $\beta 3$ integrin deficient animals, which are protected from thrombus formation (23-24). The role of $\alpha v\beta 3$ in mediating binding to vitronectin and osteopontin remains still elusive in vivo, although both ECM proteins have been found in atherosclerotic plaques (25).

1.3 Role of platelet $\beta 1$ integrins

The biological significance of platelet $\beta 1$ integrins, namely $\alpha 2\beta 1$ (collagen receptor), $\alpha 5\beta 1$ (fibronectin receptor) and $\alpha 6\beta 1$ (laminin receptor), in hemostasis is still controversially discussed. Studies using conditional $\beta 1$ knock-out mice suggested a marginal role during primary hemostasis in vivo (26) and platelet adhesion in a carotid ligation model (27). In contrast, studies on $\alpha 2\beta 1$ deficient mice indicated a significant role in thrombus formation and thrombus stabilization in a ferric chlorid model (28). Furthermore these animals exhibit prolonged tail bleeding times (29) and delayed vessel occlusion after photochemical induced injury (30). During the last decades, most studies on $\beta 1$ integrins in platelets focused on collagen receptor $\alpha 2\beta 1$. For $\alpha 5\beta 1$ $\alpha 6\beta 1$ so far only one study showed a role for both receptors on thrombus formation in a carotid artery model. However this was only indirectly by using a $\alpha 2\beta 1$ knock-out mouse with an additional pharmacological blockade of $\alpha 11\beta 3$ integrins (27). A dedicated system to prove $\alpha 5\beta 1$ or $\alpha 6\beta 1$ integrin contribution to arterial thrombosis is still missing, as single receptor knock-out mice are not available.

In vitro flow chamber assays that quantified thrombus formation on fibrillar collagen or collagen containing plaque material showed as well diverse results. Experiments using whole blood from $\beta 1$ knock-out animals showed no differences in thrombus formation compared to wildtype blood (26). Penz et al. used flow chambers covered with homogenized atherosclerotic plaque material and human platelets which were incubated with $\alpha 2\beta 1$ integrin blocking or control antibodies and found no effect on aggregate or thrombus formation (31) after $\alpha 2\beta 1$ blockage. However enzymatic digest of collagen within the plaque material leads to reduced thrombus formation, to a similar extend as seen after GPVI inhibition by usage of a blocking antibody. In summary this data underlined the importance of GPVI as main collagen signaling receptor to induce thrombus formation.

Another study using blood from $\alpha 2\beta 1$ or GPVI depleted animals showed an importance of either receptor on thrombus formation in flow chamber assays (29). Further, this group found prolonged tail bleeding times in GPVI or $\alpha 2\beta 1$ receptor depleted mice. Pugh et al. used flow chambers covered with receptor specific substrate peptides or peptide mixtures, that recognize either GPVI (substrate: CRP), $\alpha 2\beta 1$ (substrate: GFOGER) or GPIb (substrate: vWF) (32). Additionally, this

group performed all experiments under different shear conditions, as different molecular mechanisms are thought to mediate platelet activation and adhesion at different shear rates. This study verified in an elegant way that at low shear rates of 100/s or 300/s both GPVI and $\alpha 2\beta 1$ were required for thrombus formation. Whereas at a shear rate of 1000/s, GPIb and either of both collagen receptors was required and at even higher rate of 3000/s GPIb and GPVI were sufficient with only little contribution of $\alpha 2\beta 1$. Taken together, the in vitro data of above mentioned studies are rather conflicting and conclusive explanation for differences between the results are missing.

1.4 Integrin activation and the role of talin and kindlin

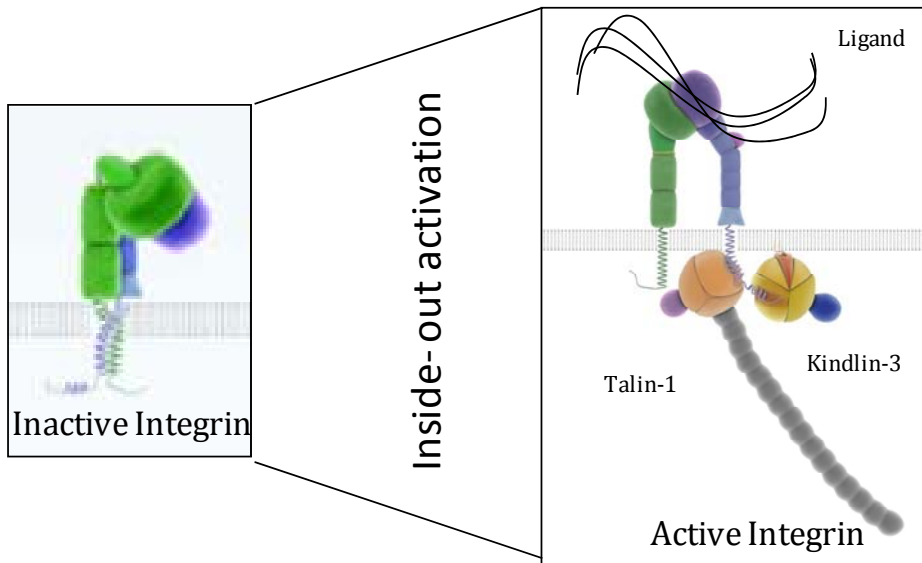
A hallmark of integrins is their ability to shift between an active and inactive conformation, which is controlled by intracellular signaling events. A tight control of integrin activity is a prerequisite for many cellular processes and is particularly important for platelets as defective or pathological activation of platelet integrins results in hemorrhages or thrombosis, respectively. Therefore integrins are found in an inactive conformation on resting platelets, but become rapidly activated when platelets get in contact to damaged vessel walls. It has been recently shown that integrin activation is under the control of two cytoplasmic protein families, talins (33) and the more recently described family of kindlin proteins (*Supplementary figure 2*).

Kindlins represent a novel family of three FERM domain proteins: kindlin-1 to 3. Historically, a mutation in kindlin-1 was identified as cause of Kindler syndrome, a rare genodermatosis characterized by an epithelial cell adhesion defect and a dermal presentation of poikiloderma and skin atrophy (34). While kindlin-1 and 2 are more widely expressed, kindlin-3 expression is restricted to the hematopoietic system. Recent in-vivo studies showed that absence of either kindlin-3 (35) or talin-1 (36-37) leads to a severe bleeding phenotype in mice due to impaired platelet integrin activation (8).

Talin and kindlin share a structurally conserved FERM domain (4.1-Protein (Four-point-one), Ezrin, Radixin, Moesin), which locates N-terminal and consist of four subdomains (F0-F3) in talin-1. In kindlin-3 it is C-terminal and comprises three subdomains (F1-F3) (33). The physical interaction to integrin cytoplasmic tails is

mediated via the F3 subdomains, which harbor a phosphotyrosine-binding domain (PTB). A structural feature of kindlin proteins is an inserted pleckstrin homology domain within the F2 domain, which mediates binding to phosphoinositides found at the inner side of the plasma membrane. Further, additional interaction sites exist and locate around the F3 subdomain in each protein and might regulate the differential recruitment of talin and kindlin to the integrin tail (see below) (33).

In-vitro pulldown experiments, using recombinant bacterial expressed cytoplasmic integrin tails revealed direct interactions of talin and kindlin with two NPxY motifs within the cytoplasmic domains of $\beta 1$, $\beta 2$ and $\beta 3$ integrins (35, 38). While the talin binding site was mapped to the membrane proximal NPxY motif, kindlins interact with the membrane distal NPxY motif. Further mutation analyses showed that the kindlin binding site extends more N-terminally and includes a double threonine motif and a serine/threonine motif within $\beta 1$ and $\beta 3$ integrins (35), respectively. This site is flanked by the two NPxY motifs and is not required for talin binding. It has been shown previously that disruption of the talin-1 binding sites within the $\beta 3$ integrin cytoplasmic domain results in an integrin $\alpha 11\beta 3$ activation defect and thrombosis resistance in mice (37). The molecular mechanism how kindlin-3 mediates its essential role during integrin activation in cooperation with talin is not known yet (34). Moreover, it was recently suggested that integrin activation can occur in the absence of kindlins and impaired integrin activity in kindlin mutant cells is due to so far unknown cellular functions of kindlin proteins (33, 39).



Supplementary figure 2: Integrin inside-out signalling (activation). Upon platelet activation, recruitment of talin-1 and kindlin-3 to the cytoplasmic tail induce a conformational shift within the integrin molecule which exposes a ligand binding site within the extracellular domain (adapted from Moser et al.(34))

1.5 From platelet activation to integrin activation

As soon as platelets are activated, a machinery of signaling cascades is induced that finalize in integrin activation. Irrespective of the initial stimulus (almost) all signaling cascades merge at the step of phospholipase activation (6). PLC2 γ facilitates the enzymatic cleavage of plasma membrane phospholipids (Phosphatidyl 4,5 biphosphate), leading to the production of IP₃ (Inositol-triphosphate) and DAG (Diacylglycerol). Both molecules act as 2nd messengers and trigger increased intracellular Ca²⁺ levels through Ca²⁺ release from endoplasmatic reticulum and subsequent opening of plasma membrane Ca²⁺ channel Orail 1 (store-operated Ca²⁺ entry (SOCE)). Elevated calcium level and increased concentration of DAG activate CalDAG-GEF1 that functions as Guanosin nucleotide-exchange-factor for Rap 1 (Ras- related protein). Rap-1 is a small G-protein of the Ras family which once GTP loaded by CalDAG-GEF1 recruits the adapter protein RIAM (Rap1–GTP-interacting adapter molecule). Genetically depleted knock-out mice for CalDAG-GEF1 and Rap 1 exhibit severely

compromised platelet aggregation and thrombus formation (40-41). Beside CalDAG-GEF1, some PKC family members feature the ability to translate increased intracellular Ca^{2+} and DAG levels into an even more sustained Rap1 activation (42).

Once established, the Rap-1-RIAM complex accompanies talin on its way to the integrin cytoplasmic tail at the plasma membrane. At the integrin tail, talin-1 destabilizes the interaction between the integrin α - and β -subunit, which will lead to the separation of the subunits. The precise temporal and spatial resolution of talin and kindlin binding to the integrin cytoplasmic domain is still under investigation. Two models in which talin-1 and kindlin-3 bind either in a parallel or sequential manner are hypothesized (34).

At this stage integrins become structurally activated by a mechanism which transmits the cytoplasmic protein binding step (43) into a conformational change throughout the plasma membrane, to open up the extracellular binding site. A structural study on $\beta 3$ integrins showed that binding of talin disrupts a stabilizing salt-bridge between αIIb residue R995 and $\beta 3$ integrin residue D723 (44). The physical separation induces a dissociation of both integrin subunits (45-46), that leads to a rearrangement of the transmembrane domain (33) as well as switchblade like extension of the extracellular domain (47). A study, using recombinant expressed and artificially linked integrin dimers showed that cleaving an introduced C-terminal clasp between both integrin subunits will lead to separation of both cytoplasmic subunits by 14nm yielding an activated ligand binding form of $\alpha 5\beta 1$ integrin receptors (48). However, the physical mechanism is still under investigation and might depend on more complex structural arrangements.

1.6 Clinical relevance of kindlin-3 in leucocyte adhesion deficiency type III

Recently, it was shown that mutations in the human kindlin-3 gene are responsible for Leukocyte adhesion deficiency type III (LAD-III) (54-55). LAD-III is a rare inherited immunodeficiency disease, which is caused by defective integrins on hematopoietic derived cells. The patients suffer from a severe bleeding phenotype and recurring bacterial infections, as all platelet and leukocyte integrins show

defective integrin inside-out signaling. Interestingly a similar phenotype is found in kindlin-3 knock out animals.(35)(49).

1.7 Clinical relevance of $\alpha 2\beta 1$ integrins in arterial thrombosis

From a historical point of view, it was known that the $\alpha 2\beta 1$ surface expression level in humans (50) vary at least around four fold. Kunicki et al. showed that increased surface expression correlates with increased adhesion to collagen, binding of fibronectin (via $\alpha 5\beta 1$ integrin) and shorter lag times during collagen induced aggregation. Worth mentioning, as soon as the aggregation was initiated, a similar maximal aggregation was reached irrespective of the surface expression level. Further studies revealed that a polymorphism at base pair 807 and 873 within the $\alpha 2$ gene correlates with different surface expression levels. Thereby, the linked polymorphism of T 807 / A 873 has higher $\alpha 2\beta 1$ expression levels compared to C 807/ G 873 (51). A first case control study by Moshfegh et al. (52) showed that patients carrying the T 807/ A 873 polymorphisms within the $\alpha 2$ gene have a higher risk of myocardial infarction (or stroke) (53) compared to controls. In contrast, a meta-analysis including 6414 cases and 7732 control patients from 14 studies (1999-2003) with a myocardial infarction or coronary stenosis as primary endpoint, failed to show a significant correlation between the T807 polymorphism and the incidence of both endpoints (54). A similar results was found in a meta-analysis on stroke patients (55).

Another study focused on patients receiving coronary intervention and stent implantation, which leads to a severe vessel wall damage due to catheter intervention. The impact of T807 polymorphism in this clinical setting was analyzed in a large retrospective study (56). Von Beckenrath et al. observed 1797 patients after coronary artery intervention and stent implantation for the appearance of acute events such as death, myocardial infarction or urgent target vessel revascularization for a follow up period of 30 days. The investigators could not find any significant adverse outcome in patients carrying the T 807 polymorphism irrespective if patients were hetero- or homozygous for this polymorphism.

Today, it is general accepted that increased surface levels of $\alpha 2\beta 1$ are no risk factor for arterial thrombotic events. However, all clinical studies were neither

designed to prove nor to reject the hypothesis that $\beta 1$ integrins contribute to arterial thrombotic disease. This is due to several limitations. First, to the best of our knowledge there are no patients reported who lack $\beta 1$ integrins in platelets. Second, evidence from clinical studies, in which the $\alpha 2\beta 1$ integrin is inhibited, is missing as no $\alpha 2\beta 1$ blocking agent is approved for clinical usage.

2. Aims of the study

First, we would like to gain more insights into the fundamental understanding of integrin-kindlin interactions. Kindlin-3 is required to activate integrins in platelets. However, so far it remains unclear if integrin inside-out-signaling requires a direct integrin-kindlin-3 interaction or if kindlin-3 acts apart from integrin tails via a so far unknown mechanism. To address this question we generated $\beta 1^{\text{TAA}^-}$ integrin mice, which carry a mutation within the kindlin-3 binding site. We decided to analyze platelets from $\beta 1^{\text{TAA}^-}$ integrin animals, as platelets are either switched on or off and have to be regulated within a fraction of a second.

Second, we would like to re-evaluate the role of $\beta 1$ integrins during thrombus formation in vivo by facilitating newly generated $\beta 1^{\text{TAA}^-}$ and β^{Hpm^-} mice. The role of platelet $\beta 1$ integrins during arterial thrombus formation in mice is still controversially discussed, ascribing $\beta 1$ integrins a rather minor/unimportant role. We would like to discriminate between the adhesive and the signaling functions of $\beta 1$ integrins. Thereby we focus on collagen induced platelet responses.

3. Materials and Methods

3.1 Animal work

3.1.1 Genetics

All mice were generated in the laboratory of Prof. Reinhard Fässler at the Max-Planck Institute of Biochemistry in Munich. All animal experiments were carried out in accordance to the German Animal protection law. All used strains and knock-out strategies are published elsewhere (see below). As $\beta 1$ integrin null animals are not viable (13), we decided to use a conditional $\beta 1$ integrin mouse (57). To allow blood cell specific gene deletion, the conditional $\beta 1$ integrin mouse was crossed with an MxCre recombinase carrying mouse. Recombinase expression is regulated by the Mx-1 promoter, which is switched on in the presence of interferon and will remove the DNA between 2 introduced recombinase recognition sites (58). In our model, interferon production is triggered by an intraperitoneal application of poly I(losine):C(Cytidine) that forms a synthetic RNA double strand. Once applied, poly I:C is recognized by toll- like- receptors and triggers an immune response, usually found after viral infections (59). Hypomorph allele carrying mice were earlier generated in our lab and published before (60). The mutant $\beta^{TTAA/-}$ mouse was generated by Dr. Hannelore Meyer and Dr. Markus Moser and will be extensively characterized in another ongoing study. Briefly, the coding region of the integrin cytoplasmic tail localizes to the last both exons of the $\beta 1$ integrin gene, exon 15 and 16. Thereby exon 16 codes the C- terminal 21 amino acids including both NPXY motifs and the double threonine 788/789 motif. A site directed mutagenesis within both threonine coding triplets replaced an adenosine-base pair against a guanine-base pair at the first position, thereby changing the aminoacid sequence from Thr 788/789 to Ala788/789. The precise cloning strategy will be published elsewhere, and is beyond the scope of this work. Interestingly, homozygous $\beta 1^{TTAA/TTAA}$ and $\beta 1^{Hpm/Hpm}$ animals are not viable as no homozygous animals were born ((60), unpublished). As one functional $\beta 1$ allele is sufficient to yield normal and healthy animals (13), we crossed heterozygous $\beta 1^{TTAA/+}$ or $\beta 1^{Hpm/+}$ animals with $\beta 1^{flox/flox}$ MxCre animals to yield $\beta 1^{TTAA/flox}$ MxCre or $\beta 1^{Hpm/flox}$ MxCre animals. Therefore, we were able to bypass embryonic lethality and to generate mice with

only one mutated $\beta 1^{TTAA/-}$ MxCre or $\beta 1^{Hpm/-}$ MxCre allele after MxCre induction by poly I:C injection.

3.1.2 Genotyping of animals

For genotyping, DNA from the tail of 4 week old mice was isolated. At day one, 1 mm of the tail tip was cut and incubated over night in 500 μ l lysis buffer. At day two, the incubation tube was centrifuged at maximal speed for 10 minutes. The supernatant was transferred into an equal volume of isopropanol. The tube was shaken until DNA precipitates were seen. Next the tube was centrifuged again at max. speed for another 10 minutes. The supernatant was carefully removed and the DNA pellet was washed with 2 ml 70% ethanol to remove remaining isopropanol. After a third centrifugation step at maximal speed for 10 minutes, the supernatant was discarded and the pellet was air dried and resuspended in 150 μ l TE buffer.

Tail lysis buffer: 50 mM Tris (pH=8.0), 100 mM EDTA, 0.5% SDS, 1:100 Proteinase K (10 mg/ml proteinase K)

TE Buffer: 10 mM Tris HCl pH 8.0, 1 mM EDTA

For genotyping the following PCR reaction mix (20 μ l final) was prepared: 2 μ l 10x PCR buffer (Metabion), 0.6 μ l 50 mM $MgCl_2$ (Metabion), 10 mM dNTP (Sigma-Aldrich), 0.2 μ l Primer forward, 0.2 μ l Primer reverse, 0.3 μ l Taq- polymerase (homemade by Dr. Moser).

Genotyping PCR primer (Metabion):

MxCre Recombinase forward : 5'-TTC-GGA-TCA-TCA-GCT-ACA-CC-3'

MxCre Recombinase reverse : 5'-AAC-ATG-CTT-CAT-CGT-CGG-3'

$\beta 1$ integrin forward: 5'-GGG-TTG-CCC-TTC-CCT-CTA-G-3'

$\beta 1$ integrin reverse: 5'-GTG-AAG-TAG-GTG-AAA-GGT-AAC-3'

$\beta 1^{TTAA}$ forward: 5'-AGC-TGT-AAA-GGT-TCT-GTG-TGG-3'

$\beta 1^{TTAA}$ reverse: 5'-CCA-AAA-CTA-CCC-TAC-TGT-GAC-3'

$\beta 1^{\text{Hpm}}$ forward: 5'-TGC TCT CAG TAA TGT TTC ATA AC-3'
 $\beta 1^{\text{Hpm}}$ reverse: 5'-GTC CTA CTG GTC CCG AC-3'

Following PCR program was used:

Step 1 95°C for 5 min
Step 2 95°C for 30 sec
Step 3 58°C for 30 sec
Step 4 72°C for 5 min
34 cycles of Step 2-4
Step 5 72°C for 5 min
Step 6 4 °C

To visualize PCR products, 5 μ l of 6x loading dye were added to PCR reactions and then loaded on a 2% agarose gel (containing 0.01% ethidium bromide) and separated by applying a current of 100 V. To visualize PCR products, gels were placed under a UV-light source and pictures were taken using an Olympus camera system.

Loading dye 10x (50ml): 30% glycerol, 100 mg of Orange G (Sigma- Aldrich), water

3.1.3 Generation of bone marrow chimeras

Femurs were isolated from adult mice and the bone marrow compartment was flushed out. Next, cells were rinsed through a cell strainer to remove cross-contaminant tissue pieces, counted and placed on ice. Next 4×10^6 cells were injected into the tail vein of two times lethally irradiated (7 Gray each) 8 weeks old recipient C57BL/6 mice. Three weeks after bone marrow transfer, mice were injected twice (day 0 and day 2) with poly I:C (GE Healthcare Life science) to induce MxCre mediated conditional knock-out. After two weeks platelets were isolated from isoflurane narcotized animals by retro-orbital plexus puncture and $\beta 1$

integrin surface expression was analyzed by flow cytometry to check knock out efficiency.

3.1.4 Carotid ligation model

This data set was generated with the help of Verena Barocke (Deutsches Herzzentrum München), who performed all experiments following the protocol described by Massberg et al. (61). Briefly, carotid arteries of anesthetized mice were dissected and ligated for 5 min by a small suture. To visualize single platelet adhesion, fluorescently DCF (Invitrogen Molecular Probes) labelled platelets (ca. 10% of platelets) from donor mice were infused and amount of adherent cells at the lesion quantified. As carotid ligation experiments were performed on different days for different groups, adherent platelet counts were expressed as percentage of adherent cells at 5 min time point in wildtype mice (which were taken as controls in every set of experiment).

3.1.5 Bleeding time assay

Mice were anesthetized with isoflurane and placed on a 37°C heating pad. All experiments were performed in a steady state narcosis with constant gas flow, monitored by breathing frequency. Next, an 8 mm segment of the tail tip was cut off, so that arterial bleeding was visible. The bleeding tail was immediately placed into 37°C warm PBS. The time until the bleeding vanished was measured. All experiments were stopped latest after 15 min by cauterization to prevent death.

3.2 Protein work

3.2.1 Bacterial transformation and bacterial culture

1st day: 50 µl of competent BL 21 bacteria were incubated with 5ng of the designated DNA plasmid for 30 min on ice, to allow plasmid binding towards the cell surface. In a next step, the reaction tubes were transferred for 90 sec on a 42°C shaker. The heat shock facilitates plasmid translocation towards the inside of the cell. After 90 sec the tubes were immediately transferred on ice to seal the

bacterial membrane. 500 µl of LB medium were added and bacteria were incubated at 37°C under shaking conditions for at least 60 min and then dispersed on an agar plate containing 50 µg/ml of ampicillin (at 37°C).

2nd day: bacterial colonies were picked from each agar plate by the help of a pipette tip and transferred into 100 ml LB (50 µg/ml ampicillin) preculture and incubated at 37°C under shaking conditions. 3rd Day: 50 ml of preculture were transferred into 1 l LB (with 50 µg/ml ampicillin) medium and grown until the optical density at 600 nm reached 0.6. Next, IPTG (isopropyl-beta-D-thiogalactopyranoside) with a final concentration of 1mM was added to induce protein expression. After 5 h bacteria were harvested by centrifugation at 2500x g for 30 min at 4°C.

LB Medium (1l): 25 g yeast extract, 50 g trypton, 50 g NaCl

3.2.2 Integrin tail peptide production

The plasmid carrying the designated integrin tail sequence linked to 10 His residues in a Pet-16b cloning construct was kindly provided by David Calderwood. The following pulldown experiments used Nickel loaded agarose beads to bind the histidine tag. A disadvantage of highly charged nickel beads is the remaining unspecific background binding of proteins within the reaction batch that will contaminate the pulldown experiment. To circumvent this drawback we decided to redesign the integrin full length cytoplasmic tails to switch to a biotin (tag) streptavidin (magnetic bead) system. Therefore, we introduced a cysteine residue, three amino acids upstream of the cytoplasmic integrin tail coding region. The plasmid mutation work was done by a two step mutagenesis using a strategene quick mutagenesis kit following manufactures instructions (Primer: Step 1 forward: AGC GGC CAT ATC GAA GGT CGT CAT ATG TGT GGG CCC AAG CTT TTA ATG ATA ATT CAT, Step 1 reverse: ATG AAT TAT CAT TAA AAG CTT GGG CCC ACA CAT ATG ACG ACC TTC GAT ATG GCC GCT, Step 2 forward: ATC GAA GGT CGT CAT ATG CTG GAA GTT TGT GGG CCC AAG CTT TTA ATG ATA ATT CAT, Step 2 reverse: ATG AAT TAT CAT TAA AAG CTT GGG CCC ACA AAC TTC CAG CAT ATG ACG ACC TTC GAT). Mutated plasmids were transfected into XL-1 bacteria and grown over night. Next day colonies were

picked, transferred into mini cultures and grown over night. The day after, a Quiagen mini-prep set (Quiagen was used to isolate DNA plasmid from bacterial cultures, before sending plasmids to the Max-Planck–core unit for sequencing.

3.2.3 Protein purification

Bacteria pellets were washed in buffer A. As integrin tail peptides accumulate in bacterial inclusion bodies, bacteria were lysed with 8 M Urea containing buffer B on ice and additionally sonicated at maximal power for six times 15 sec each. Next, the lysate was centrifuged for another 30 min at 20000x g. Supernatants were incubated with 2ml of freshly prepared nickel loaded NTA-resin beads for 2 h on a rotator at room temperature. After washing with Buffer B, integrin tails were eluted by addition of 2 ml of elution buffer. In a next purification step proteins were loaded on a reversed phase HPLC (C-8 column, eluted by an acetonitril gradient in 0.08% TFA (tri-flour-acid) as carrier medium and aliquoted. Following a 2 hours vacuum centrifugation at 50 g at 37°C to evaporate the acetonitril, aliquots were lyophilized under high vacuum over night. The peptide powder was resuspended in steril PBS (ph 7.4). The biotinylation of the cysteine residue was performed as recommended by instructors guide (Pierce: EZ-Link NHS-SS-Biotin Kit). The reaction mixture was then purified by a size exclusion column (Vivaspin 3000) centrifugation step (30 min at 400g). The resulting peptide solution was kept under reducing conditions in the presence of β - mercaptoethanol at 4°C, until used.

Buffer A: 150 mM NaCl, 1 mM EDTA, 10 mM Tris, pH 8

Buffer B: 150 mM NaCl, 1 mM EDTA, 10 mM Tris, 8 M urea, pH 8

Elution buffer: 50 mM imidazole in buffer B

3.2.4 Protein concentration determination by Bradford assay

Protein concentration was determined, by the so called Bradford method, using Bradford reagent (Sigma-Aldrich). This method is based on the different light absorption of Coomassie blue dye as it binds to protein. Unprotonated Coomassie blue dye binds non-covalently to positively charged amino acid residues (e.g.,

arginin, lysine, histidine) and will increase light absorption at λ 620nm in contrast to the protonated unbound form.

3.2.5 UV spectroscopy to determine protein concentration

This method is based on the Beer–Lambert-law, which states that the amount of protein is proportional to the light it absorbs. Aromatic side chains containing amino acid such as tryptophan, tyrosine and phenylalanine absorb UV light at a wavelength of 280 nm. Each protein has a specific light extinction coefficient (L/mol x cm) which can be calculated (e.g. by Peptide property Calculator of the Northwestern University, USA). To calculate the concentration the Beer Lambert law: $A = \epsilon c l$

Is adapted as followed: $c = A / \epsilon l$

(A absorbance, ϵ extinction coefficient, l path length of the cuvette (cm))

3.2.6 Pulldown assays

50 μ g Biotin-fusion proteins were incubated with fresh platelet lysates in PD buffer for 4 h. Magnetic-Streptavidin labeled Dynalbeads (Invitrogen) were added for 30 min and then pulled out by using a magnet. Beads were washed three times with 0.5 ml PD buffer, boiled in 2x Laemmli buffer and subjected to immunoblotting. Tail loading was visualized by Coomassie staining.

PD buffer: 150 mM NaCl, 50 mM Tris, EDTA 1 mM, Triton-X 100 0.1%, Protease inhibitor tablets (Sigma-Aldrich) and phosphatase inhibitors P1 and P2 (Sigma-Aldrich), pH 7.4

2x Laemmli buffer: 4% SDS, 20% Glycin, 10% β -Mercaptoethanol , 0.004% bromphenol blue, 0.125 M Tris HCl

3.2.7 Immunoblotting

SDS-polyacrylamide gel electrophoresis allows the separation of denatured proteins corresponding to its molecular weight. For SDS gel casting, electrophoresis and western blotting (of proteins on a PDVF membrane) a BIO-RAD system was used. First, a 10% resolving gel was casted (volume 10 ml: 4.0 ml water, 3.3 ml of 30% acrylamid mix, 2.5 ml 1.5 M Tris (pH 8.8), 0.1 ml 10% SDS, 0.1 ml 10% ammonium persulfate, 0.006 ml TEMED), second a stacking gel (volume 5 ml: 3.4 ml water, 0.86 ml of 30% acrylamid mix, 0.63 ml 1.0 M Tris (pH 6.8) 0.05 ml 10% SDS, 0.05 ml 10% ammonium persulfate, 0.006 ml TEMED) was prepared and a loading comb was inserted. Gels were placed into a SDS running buffer filled chamber. Samples containing a final volume of 1x Laemmli buffer were boiled for 5 minutes at 95°C, loaded into comb pockets and separated by a current of 40 mA. Next, the gel is placed on top of an isopropanol rinsed PDVF (polyvinylidene-difluoride, BIO-RAD) membrane, which is covered by 3 layers of whatman paper at the back and front side of the gel-membrane “sandwich”. The “sandwich” is placed into a blotting chamber filled with blotting buffer and proteins were transferred onto the membrane by applying a current of 240 mA. Subsequently, membranes were blocked with 2.5 % milk powder dissolved in TBST buffer to saturate unspecific binding sites before primary antibodies were added over night for incubation. At the next day, the membrane was washed 3 times for 15 minutes with TBST, and corresponding secondary HRP (horse radish peroxidase) coupled antibodies were incubated for 1h at room temperature. After a second TBST wash (three times for 15 min) the membrane was incubated with a developing solution (Amersham: ECL- kit). The horse radish peroxidase generated chemi-luminescence signal was detected with a high sensitive photo film (Amersham Hyperfilm) and then developed in an appropriate film developing machine (Kodak).

Running buffer (1l): Tris-base 3.03 g, glycine 14.4 g, SDS 1.0 g in H₂O

Blotting buffer (1l): glycine 28.8 g, Tris base 6.04 g, methanol 200 ml, ddH₂O 1.6 L

TBST buffer (1l): Tris 1.21 g, NaCl 8.76 g, Tween-20 0.5 ml

Following antibodies were used:

Protein	Species	Vendor	Catalog number	WB concentration
FAK (Phosphorylated - Y397)	rabbit	Biosource	#44-624G	1:1000
FAK	rabbit	Upstate	06-543, 21819	1:1000
Talin-1 (C-20)	goat	Santa Cruz	sc-7534	1:1000
Integrin beta 1	rat	Chemicon	MAB1997	1:1000
Kindlin-3	rabbit	Moser et al.		1:5000
GAPDH	mouse	Calbiochem	CB1001	1:30000
Anti- Ig goat- HRP	mouse	Jackson	205-032-176	1:10000
Anti- Ig mouse- HRP	goat	Jackson	115-035-174	1:10000
Anti- IgG rabbit- HRP	mouse	Jackson	211-032-171	1:10000
Anti- Ig rat – HRP	donkey	Jackson	712/035/150	1:10000

3.2.7.1 Stripping of western blot

To re-probe blotting membranes with another primary antibody, membranes were incubated with stripping buffer for 30 min at 55 °C. After washing twice with TBST for 15 min, membranes were re-blocked with milk-TBST solution and processed as described above.

Stripping solution: 2% SDS, 62.5 mM Tris pH 6.8, freshly added β -Mercaptoethanol (360 μ l in 50 ml)

3.2.7.2 Coomassie staining

SDS gels were briefly rinsed in water before transferred into Coomassie staining solution. Gels were stained for 1 hour. Protein bands were visualized after placing the gel into destaining solution.

Coomassie staining solution: 50% methanol, 10% acetic acid, 40% water and 0.25% Coomassie blue R250.

Destaining solution: 10% acetic acid in water.

3.2.8 Integrin phosphorylation analysis

Washed platelets were incubated in 100 μ l Tyrodes buffer (without phosphate) pH 7.4 for 30 min at 37 °C in the presence of 50 nM Calyculin A. Next, platelets were stimulated with 0.1 U/ml Thrombin. After 60 sec, an equal volume of 2x Laemmli buffer was added and the sample was immediately boiled for 5 min at 95°C. Boiled samples were subjected to SDS gel electrophoresis (8% gel) and Coomassie stained. The band corresponding to the molecular weight of β 1 integrin was cut out and sent to non-quantitative phospho-massspectrometry analysis at Max-Planck Institute of Biochemistry core unit in Martinsried.

3.3 Platelet work

3.3.1 Platelet isolation

Mice were anesthetized by isofluran inhalation and blood was drained from the retro-orbital plexus into 200 μ l 20 U/ml Heparin- TBS, by using Heparin (Sigma-Aldrich) rinsed capillaries. Blood was centrifuged twice at 75x g and 100x g respectively, in a tabletop centrifuge (Eppendorf) for 10 min in soft acceleration/deceleration mode. Erythrocyte depleted serum was transferred into a new tube and then spun down by centrifuging for 5 min at 1500x g. After two washing steps with Tyrodes buffer pH 6.5, the platelet pellet was suspended in Tyrodes buffer pH 6.5 and the platelet concentration was determined using a Hemovet blood counter (Hemovet, Germany).

Tyrode's buffer (without phosphate): 137 mM NaCl, 2.8 mM KCl, 12 mM NaHCO₃, 5.5 mM glucose and 10 mM Hepes, pH6.5 or 7.4, \pm 1 mM MgCl₂, \pm 1 mM CaCl₂, \pm 1 mg/ml BSA

3.3.2 Flow cytometry

Platelets were isolated and incubated with the desired fluorophore-conjugated antibodies for 15 min at room temperature and then directly analyzed on a FACScalibur flow cytometer (Becton Dickinson). For activation assays, platelets were stimulated for 15 min with the indicated agonists (Thrombin (Sigma- Aldrich), Convulxin (Alexis), ADP (Alexis), U46619 (Alexis)) and immediately analyzed.

Following antibodies were used:

Protein	Dye	Source	Clone	Vendor	Conc.
Integrin β 1 (CD29)	PE	Hamster IgG	HMBeta1-1	BioLegend	1:200
Integrin β 3 (CD61)	PE	Hamster IgG	2C9.G3	eBioscience	1:200
Integrin α 2 chain (GPIa)	FITC	Rat IgG2b	Sam.G4	Emfret	1:200
GPVI	FITC	Rat IgG2a	JAQ1	Emfret	1:200
GPIX (CD42a)	FITC	Rat IgG1	Xia.B4	Emfret	1:200
CD62P (P-selectin)	FITC	Rat IgG1	Wug.E9	Emfret	1:200
Active integrin α IIb β 3	PE	Rat IgG2b	JON/A		1:200
IgG2a rat isotype ctrl	FITC	Rat IgG2a		NatuTec	1:200
IgG2b rat isotype control	FITC	Rat IgG2b	TBE 15	EuroBiosciences	1:200
IgG1 rat isotype control	PE	Rat IgG1	R3-34	PharMingen	1:200
IgG hamster isotype con.	PE	Hamster IgG	HTK888	BioLegend	1:200

3.3.3 Platelet spreading

Glass slides were coated with 1 mg/ml fibrinogen (Sigma) or 25 μ g/ml acid soluble collagen I (Sigma- Aldrich, Collagen I from rat tail) overnight at 4°C. At day two, slides were rinsed with PBS and then blocked with 1% BSA (bovine serum albumin) in PBS for 1 h. 1.5 Mio platelets were suspended in 150 μ l Tyrodes buffer in the presence or absence of 0.75 mM Mn²⁺. Cells were stimulated with 0.1 U/ml, Thrombin (Sigma- Aldrich), immediately plated and the glass slides were incubated at 37°C. After 45 min unbound cells were washed off and DIC (differential interference contrast) microscopy was performed, using a 100x oil immersion lens on a Zeiss DIC microscope equipped with Metamorph- software. Acquired pictures were analyzed for platelet spreading size using ImageJ software and manual selection of spreading area.

PBS (1l) ph 7.4: NaCl₂ 8 g, KCl 0.2 g, Na₂HPO₄ 1.44 g, KH₂PO₄ 0.24 g, fill up with ddH₂O (double distilled H₂O)

3.3.4 β 1 integrin staining

WT cells were stimulated with 0.1 U/ml Thrombin and allowed to spread for 30 min on acid soluble collagen I coated glass slides. Next, cells were fixed for 15 min in 4% PFA in TBS. Then cells were permeabilized with 0.05% Triton X-100 TBS for 15 min. To block unspecific background binding, cells were incubated with 1% BSA in TBS for 1h. Primary antibody, anti- β 1 integrin (Chemicon, Mab 1997, 1:500) in 1% BSA containing TBS, was incubated for 1h at RT (room temperature) and secondary, goat- anti- rat, C3 labeled antibody (Jackson) was incubated for another 30 min at RT in the dark. To visualize specific binding, isotype control staining (FITC Rat isotype control, eBioscience, 1:500) was performed in parallel. Pictures were acquired using as ZEISS TIRF microscope in DIC, epifluorescence or TIRF mode, equipped with MetaMorph software (Molecular devices).

3.3.5 Aggregation assay

To determine platelet aggregation, light transmission was measured by adding 70 μ l of washed platelets (300000/ μ l) in 140 μ l Tyrodes buffer ph 7.4 in the presence or absence of fibrinogen (final concentration of 100 μ g/ml) and Mn²⁺ (final concentration of 0.75 mM), respectively. Platelets were stimulated with 1ng/ml convulxin (Alexis) or 5 μ g/ml fibrillar collagen (Nycomed). Transmission was recorded on an Aggrolink (Aggrolink Germany, Probe and go) 2 channel aggregometer over 10 minutes and expressed as arbitrary units. Thereby, 100% transmission (unstimulated cells) corresponds to 0% aggregation. A decrease in light transmission, due to platelet shape change, was expressed as negative aggregation values (-x %).

3.3.6 Fibrinogen secretion assay

Experiments were performed as described for aggregation experiments (see above) in the absence of fibrinogen and BSA. After 8 min of stirring, the reaction batch was spun down by centrifugation (14000x rpm table top centrifuge) for 30 sec and boiled in 1x Laemmli buffer. Lysates were subjected to immunoblotting for fibrinogen γ - chain. GAPDH was used as internal loading control to show equal loading. Decreases in cellular fibrinogen- γ content were quantified by densitometry (Image J software).

3.3.7 Evaluation of ATP release from dense granula

A luciferin-luciferase detection system (Promega) was used to quantify ATP release to monitor dense granule secretion. For these experiments, platelets were stimulated with 5 μ g/ml fibrillar collagen or 0.1 ng/ml convulxin in a lumino-aggregometer (Aggrolink, Germany) under stirring conditions in the presence of luciferase and its substrate luciferin. Emitted luminescence was recorded and maximal values were expressed as ratio of luminescence values from fibrillar collagen stimulate versus CVX stimulated platelets.

3.4 Statistical analysis

Significance level are calculated by a two- tailed, unlinked student's T- test, and are indicated in the figures. Error bars represent standard error mean values.

4. Results

4.1 Integrin tail-peptide production and pulldown experiments

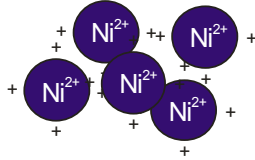
The kindlin-3 binding site at the $\beta 1$ integrin cytoplasmic tail spans the region from the membrane distal NPXY motif to the more proximal located residues including a double threonine motif. For our earlier pulldown experiments we used full length integrin tail peptides (35, 38), labeled with a hexa- histidine tag, which were pulled down by nickel loaded agarose beads. A drawback of nickel beads is a high unspecific background binding which require harsh washing conditions. We wanted to decrease background binding by using streptavidin-coupled magnetic beads for the pulldown. We redesigned genetically our tails (Figure 1) so that a biotin molecule could be coupled via a disulfide bound to an introduced cysteine residue. To test the biological activity of freshly produced tails, pulldown experiments were performed, using Streptavidin coupled magnetic beads. We found significantly less kindlin-3 binding to $\beta 1^{\text{TAA}}$ integrin than to wild type tails without affecting talin binding. Coomassie staining of the low molecular weight fraction of the SDS gel showed equal amounts of tails per reaction. Furthermore mass spectrometry of marked (asterisk) bands verified a successful integrin peptide mutation and expression (Figure 2).

β1 Integrin (wildtype) cytoplasmic tail (amino acid sequence)

W- KLLMIHDRREFAKFEKEKMNAKWDTGENPIYKSAVTTVVNPKYEGK

Integrin cytoplasmic tail expressed in Pet-16b - HIS- Tag vector

MGHHHHHHHHHHSSGHI~~EG~~RHML ~~EVLFQGP~~ KLMIHDRREE.....EGK



pulldown via Ni²⁺ charged agarose beads

Redesinged Integrin cytoplasmic tail expressed in Pet-16b HIS Tag vector

Cysteine residue is introduced at position 23

5 Residues were deleted at Pos 24-28

MGHHHHHHHHHHSSGHI~~EG~~RHM ~~CGP~~ KLMIHDRREE.....EGK

S
|
S



pulldown via magnetic streptavidin beads

Figure 1: Amino-acid sequence of β1 integrin tail and bacterial expressed peptide sequence. Bacterial expression vector (Pet-16b) residues are in green, integrin coding sequence is shown in black, the deleted residues are in orange and newly introduced cysteine residue in red. Pulldown beads interaction sides are indicated.

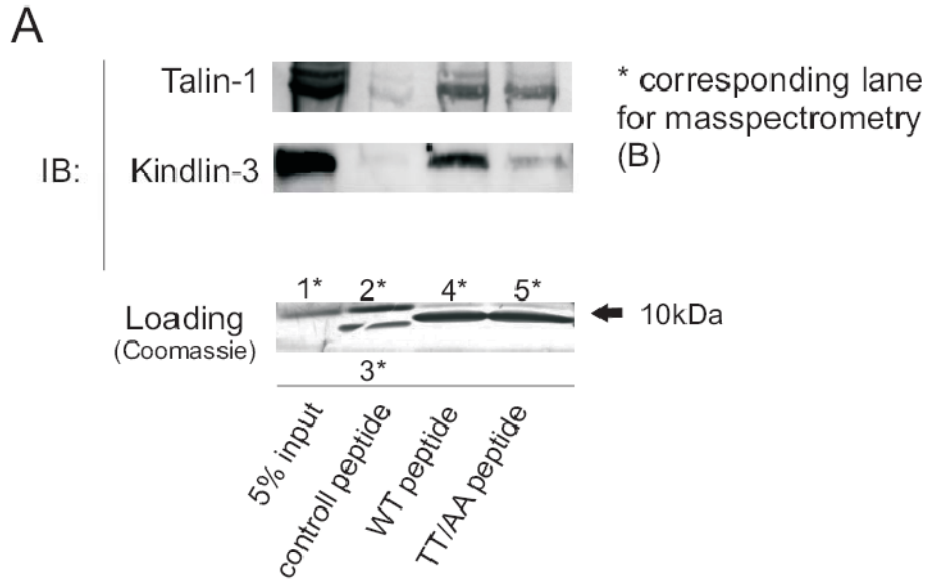


Figure 2: Pulldown experiment. Kindlin-3 binding to $\beta 1^{TTAA}$ mutated cytoplasmic integrin tail is reduced. Recombinantly expressed cytoplasmic $\beta 1$ integrin tails (WT vs. TT/AA) were incubated with WT platelet lysates. Pulldown eluates were separated on SDS gel and immuno-blotted for kindlin-3 and talin-1. Results are representative for 3 independent experiments.

4.2 Experimental design and generation of $\beta 1^{TTAA/fl}$ MxCre and $\beta 1^{Hpm/fl}$ MxCre mice

To analyze $\beta 1$ integrins lacking a functional kindlin binding site in vivo, we used mouse mutants in which the double threonine motif (TT788/789) within the $\beta 1$ cytoplasmic domain was replaced by two alanine residues (unpublished H. Meyer et al.). Mouse mutants that carry this mutation on both alleles ($\beta 1^{TTAA/TTAA}$) are not viable and their phenotype will be described elsewhere. Heterozygous mice ($\beta 1^{+/TTAA}$) are normal and were mated with conditional $\beta 1$ integrin mice ($\beta 1^{fl/fl}$), which additionally express an inducible cre-recombinase under the Mx1 promoter to obtain $\beta 1^{TTAA/fl}$ Mx1-Cre mice. Recombination and inactivation of floxed $\beta 1$ integrin yielded hematopoietic cells, with only the mutant $\beta 1^{TTAA}$ integrin expressed.

Furthermore, we included a $\beta 1$ integrin hypomorph mouse which expresses only minor amounts of (active) beta-1 integrins. As homozygous animals are also not viable, heterozygous ($\beta 1^{+/hpm}$) mice were bred and treated in parallel to mutant animals. Our experimental set up with all used mice strains is shown in Figure 3.

A

Mouse					
	WT	HT	KO	TT/AA	Hpm
$\beta 1$ Genotype	+/+	+/-	-/-	TT/AA/TT/AA	Hpm/Hpm
Viability	+	+	-*	-**	-***
Generated bone marrow chimera C57/Bl6 (12 weeks old donors)					
	WT	HT	KO	TT/AA	Hpm
MxCre	-	+	+	+	+
$\beta 1$ Genotype	+/+	+/fl	f/fl	TT/AA//fl	Hpm/fl

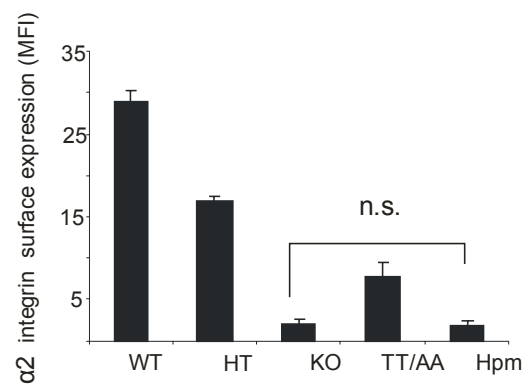
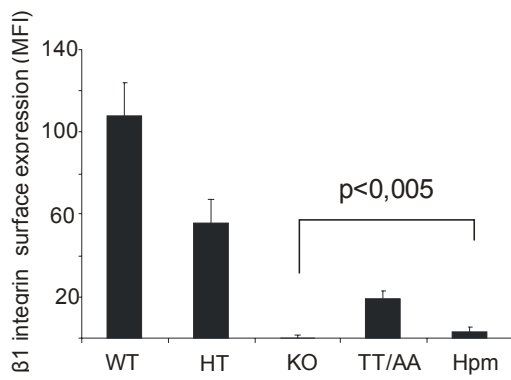
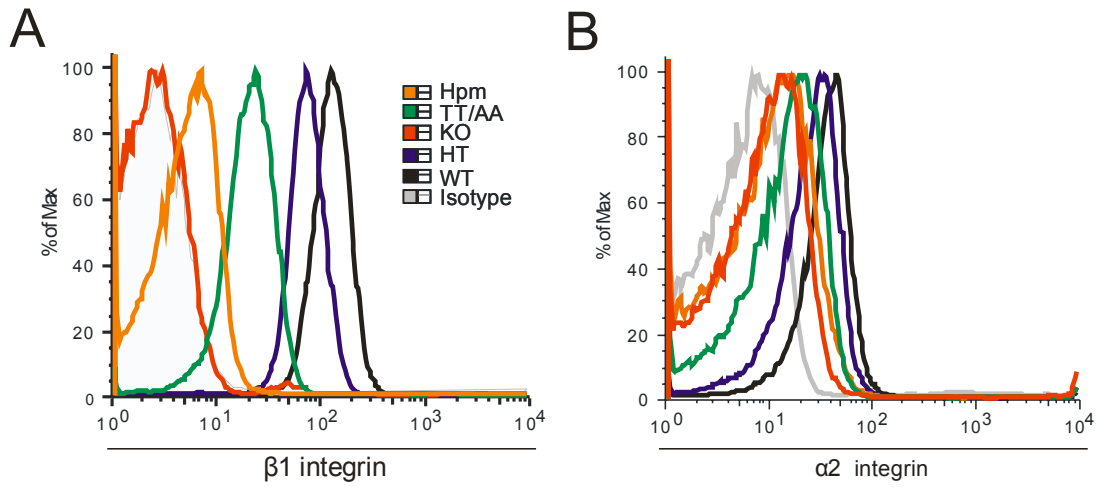
*Figure 3: Experimental design. Table-A gives an overview of the subgroups used in this study. Used mice are listed by $\beta 1$ genotype (+ WT allele, - deleted $\beta 1$ integrin allele, TT/AA-mutated allele or Hpm-hypomorph allele) and viability (+ born alive, - not born; * see text for further explanation). To bypass embryonic lethality, mice were bred into $\beta 1$ conditional background carrying a blood cell specific inducible MxCre system and utilized to generate bone marrow chimera.*

4.3 Platelet characterization

First, we isolated platelets from bone marrow chimera and asked whether the introduced ($\beta 1^{\text{TAA}}$) mutation affects $\beta 1$ integrin surface expression. Indeed, upon cre-mediated deletion of the wild-type $\beta 1$ integrin allele only 18% of mutant $\beta 1^{\text{TAA}}$ surface integrin was detected by flow cytometry in comparison to $\beta 1$ integrin levels on wild-type platelets (Figure 4A). Due to this reduction our experimental set up included inducible heterozygous ($\beta 1^{+/fl}$ MxCre) and homozygous ($\beta 1^{fl/fl}$ MxCre) conditional $\beta 1$ mice (62) (Figure 4A) as well as newly generated inducible $\beta 1$ hypomorph mice ($\beta 1^{\text{Hpm}/fl}$ MxCre) (unpublished, Figure 3) as internal controls. The latter expresses very low $\beta 1$ integrin level as a consequence of nonsense mediated RNA decay (NMD) (60). As expected, poly I:C induced Cre expression resulted in a complete absence and approximately 51% of wild-type $\beta 1$ integrin levels on platelets of $\beta 1^{fl/fl}$ MxCre and $\beta 1^{+/fl}$ MxCre mice, respectively. Platelets from $\beta 1^{\text{Hpm}/-}$ MxCre mice showed only 3,2% $\beta 1$ integrin expression level after Cre-mediated deletion of the floxed $\beta 1$ allele compared to wild-type platelets (Figure 4A).

Since the formation of functional heterodimeric integrin molecules occurs already in the endoplasmatic reticulum and only correctly formed heterodimers are transported to the plasma membrane, diminished expression of the $\beta 1$ integrin subunit caused a similar reduction in $\alpha 2$ integrin surface expression levels (Figure 4B) as well as $\alpha 5$ and $\alpha 6$ subunit expression (data not shown). In contrast, surface expression levels of $\beta 3$ integrin, GPVI and GPIX were similar between groups (Figure 4 D).

Western blot analysis from total platelet lysates also confirmed strongly reduced $\beta 1^{\text{TAA}}$ integrin expression levels indicating that the kindlin-binding site mutant $\beta 1$ integrin has either reduced stability or expression. Expression of talin-1 and kindlin-3 was not changed in platelets of all genotypes (Figure 4C).



	$\beta 1$ (MFI)	+/- SD	% Wt
WT	107,50	15,72	100
HT	55,74	11,53	51,85
KO	0,68	1,12	0,63
TT/AA	19,26	3,80	17,92
Hpm	3,48	2,45	3,24

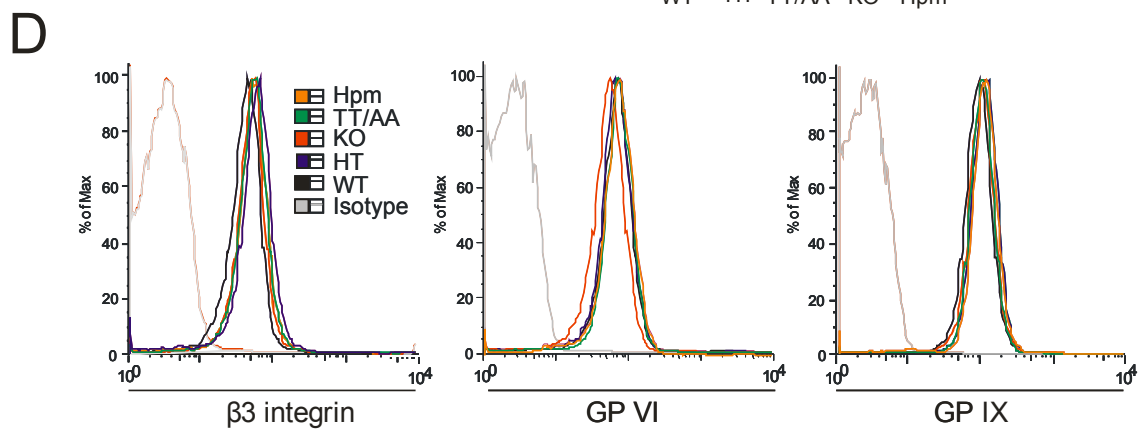
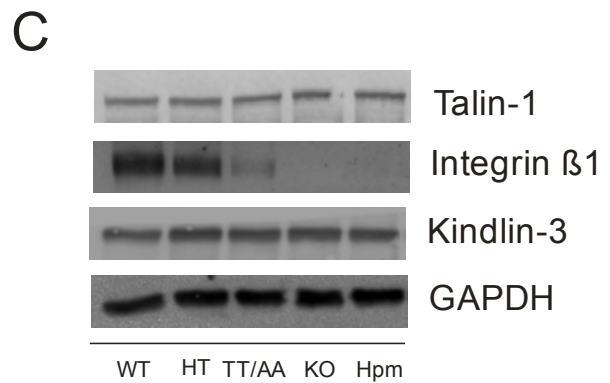


Figure 4: Characterization of platelets. Purified platelets (from $n \geq 6$ chimeric animals per group) were analyzed by flow cytometry for $\beta 1$ (A) and $\alpha 2$ integrin (B) cell surface expression. (C) To determine total protein levels, platelets were lysed and immunoblotted for $\beta 1$ integrin, talin-1, kindlin-3 and GAPDH as loading control. (D) No differences between groups were found for $\beta 3$, GPVI and GPIX cell surface expression.

4.4 Integrin activation assays

Next we wanted to test whether kindlin-binding deficient $\beta 1^{\text{TTAA}}$ integrins can shift towards an active conformation. To this end, platelets from chimeric animals of all different genotypes were isolated and activated by different agonists in vitro. Active $\beta 1$ integrins were measured by flow cytometry using the conformation specific 9EG7 antibody (63-64) that only binds to active $\beta 1$ integrins. The acquired 9EG7 values were then corrected according to the $\beta 1$ integrin surface expression levels between the groups. As shown in Figure 5A, treatment with 1ng/ml convulxin, 5 mmol thromboxane A analog U46619 or 0.1 U/ml thrombin, which all stimulate platelets via different receptor signaling pathways (6), fail to activate mutant $\beta 1^{\text{TTAA}}$ integrins. In contrast $\beta 1$ integrins on platelets from hypomorph and heterozygous mice became activated comparable to $\beta 1$ integrins in wild-type platelets. In sharp contrast, activation of the $\alpha \text{IIb}\beta 3$ integrin, as measured by conformation specific JON/A (active *$\alpha \text{IIb}\beta 3a$* integrin) antibody, was not affected in these cells (Figure 5B). These data indicate that a direct interaction between kindlin-3 and $\beta 1$ integrin is required for $\beta 1$ integrin inside-out activation in platelets.

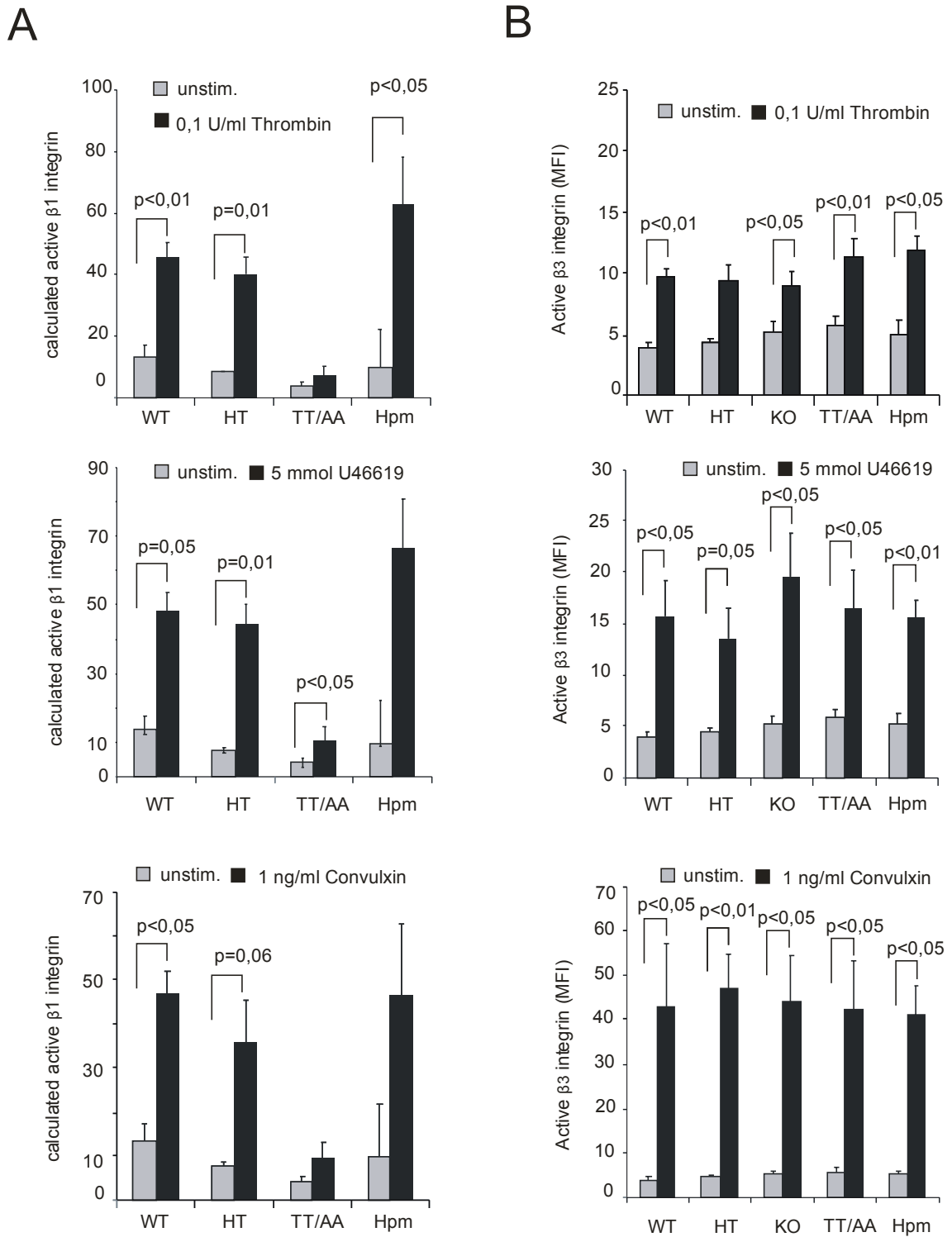


Figure 5: $\beta 1$ integrin activation is reduced in $\beta 1^{TTAA/-}$ platelets. $\beta 3$ integrin activation is unaffected. To determine $\beta 1$ integrin activation (A), platelets were stimulated with indicated agonists and 9EG7- FITC (conformational active $\beta 1$) binding was measured by flow cytometry. To adjust for different $\beta 1$ surface levels, acquired values were normalized

to 100% (WT) $\beta 1$ surface expression (see Figure 4). (B) Shown are MFI (mean fluorescence intensity) values for JON/A binding (conformational active $\alpha IIb\beta 3$ integrin) after agonist stimulation. Bars represent mean values of independent experiments ($n \geq 3$), error bars represent $\pm SEM$, significance levels are indicated. (Graphs are depicted at the following page)

4.5 Platelet spreading

Being able to show that integrin inside-out activation is defect, we ask whether a direct integrin kindlin interaction is required for outside-in signaling. Integrin signaling triggers intracellular signals that re-organize the actin cytoskeleton during cell spreading (65). To further characterize the functional properties of $\beta 1^{TTAA}$ integrins, platelet adhesion and spreading on soluble collagen or fibrinogen coated surfaces were analyzed. So far little is known about $\beta 1$ integrin distribution in spreaded platelets on acid soluble collagen. In contrast, platelets spreading on fibrinogen form a typical pan-cake like shape thereby arranging an adhesion ring established of activated $\beta 3$ integrins around the outer circumference (66). To check for $\beta 1$ distribution we stained $\beta 1$ integrins in WT platelets spread on collagen. TIRF microscopy (Total internal reflection microscopy) reveals indeed a $\beta 1$ containing adhesive ring-like structure, although cells were unable to transform into a pancake-like structure most likely due to an overall decreased number of adhesions being formed. TIRF microscopy penetration depth is limited to several hundred nanometers (up to 400nm) and it might therefore fail to visualize additional intracellular pools of $\beta 1$ integrins. To exclude an additional integrin pool, epifluorescence microscopy was performed and showed a similar distribution pattern (Figure 6).

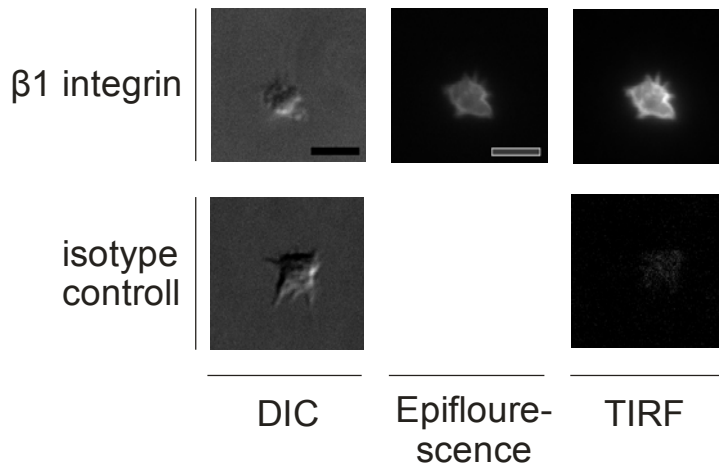


Figure 6: $\beta 1$ -integrins form an adhesive ring at the outer circumference of spread platelets. Thrombin stimulated wild-type platelets were allowed to spread for 30 min on soluble collagen and afterwards fixed and stained for $\beta 1$ integrin. Pictures were acquired in DIC (Differential interference contrast), epifluorescence and TIRF microscopy mode, respectively. Images are representative for 3 independent experiments. Scale bar relates to $5 \mu\text{m}$.

Adhesion of washed platelets was performed in the presence of 0.1 U/ml thrombin and with or without Mn^{2+} . Acidic soluble collagen I is bound by $\alpha 2\beta 1$ integrins via a repeatedly found GFOGER motif (67). This motif is not recognized by GPVI, which requires a more complex binding motif present in fibrillar collagen (68). Hypomorphic and $\beta 1$ deficient platelets showed a severe spreading defect on soluble collagen I, both in the presence or absence of Mn^{2+} (Figure 7A). These cells formed elongated filopodia and only occasionally small lamellipodia. Consistent with the defect in inside-out activation, $\beta 1^{\text{TAAV-}}$ platelets also failed to form lamellipodia and showed reduced spreading (Figure 7A). Notably, Mn^{2+} -treatment rescued the spreading defect of $\beta 1^{\text{TAAV-}}$ platelets significantly. As control all cell types were seeded on fibrinogen a $\alpha \text{IIb}\beta 3\text{A}$ integrin ligand and could spread and adhere normal. To further validate this hypothesis, we tested FAK phosphorylation as readout for integrin outside-in signaling (69). Tyrosine phosphorylation within the FAK molecule (e.g., Tyrosine 397) yield several docking sites for SH2 domain containing signaling molecules such as Src family kinases

thereby promoting cell spreading and adhesion (70-71). This time platelets were stimulated with fibrillar collagen to induce integrin inside out signaling and then seeded on soluble collagen in the presence or absence of Mn^{2+} for 30 minutes. Next, FAK phosphorylation was determined by Western blot analysis. Again, whereas $\beta 1^{TTAA/-}$ mutant platelets revealed low pFAK levels similar to $\beta 1^{-/-}$ knockout platelets, Mn^{2+} treatment resulted in an increase in pFAK levels in $\beta 1^{TTAA/-}$ platelets but not in $\beta 1^{-/-}$ knockout platelets (Figure 8).

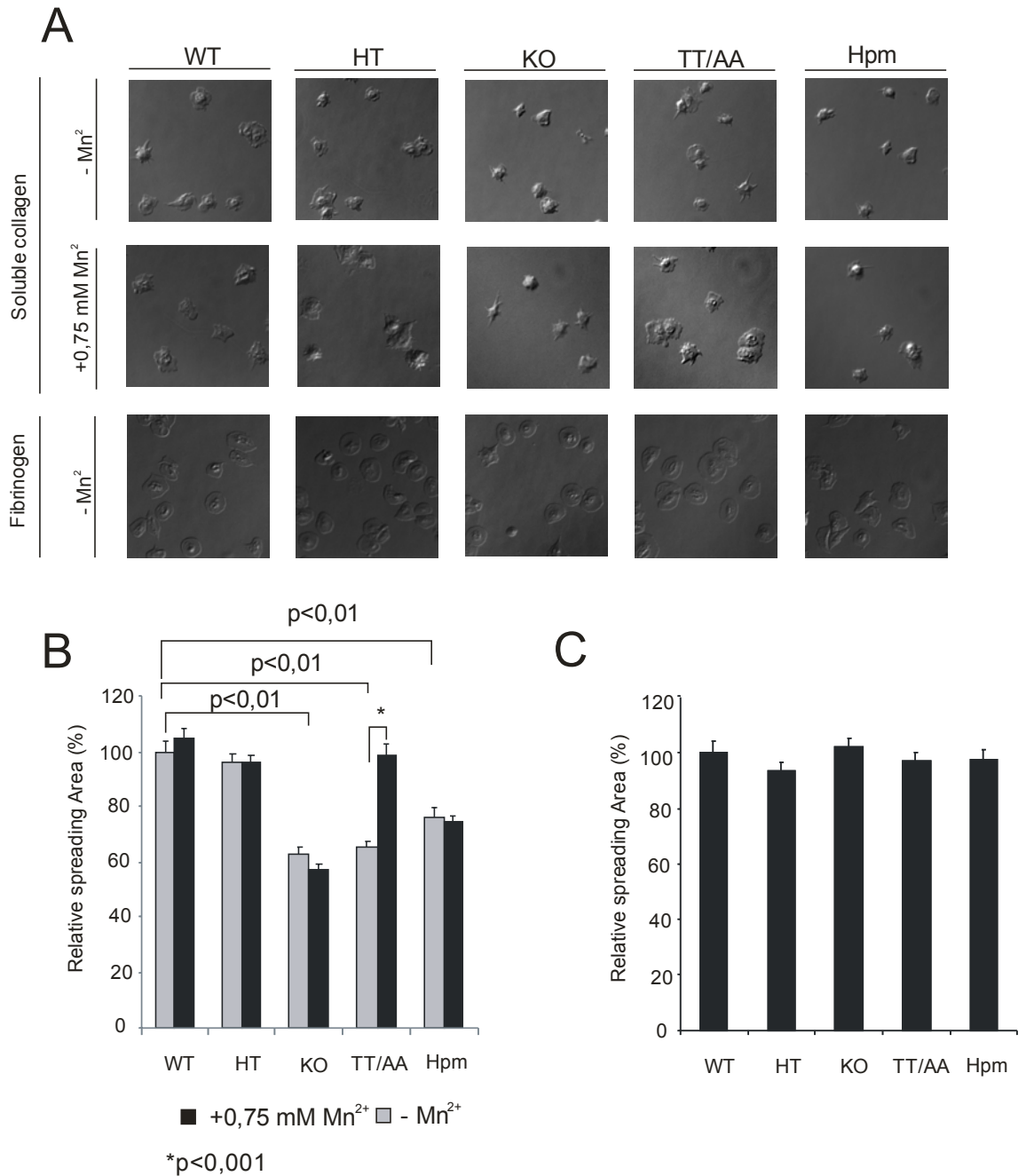


Figure 7: Spreading of thrombin stimulated platelets. Platelets (15×10^6 cells/ $150 \mu\text{l}$) were stimulated with 0.1 U/ml Thrombin and seeded on (A) acid soluble collagen I ($25 \mu\text{g/ml}$) or fibrinogen (1 mg/ml , no Mn^{2+}), in the absence or the presence of $0,75 \text{ mmol Mn}^{2+}$. After 45 min , cells in suspension were carefully washed away, DIC pictures ($100.6 \times$) acquired and spreading size measured using Image J software. Cell size of at least 100 cells was measured and quantified as % of WT cell size of spread platelets on soluble collagen (B) or on fibrinogen (C), respectively. Pictures are representative for at least 3 independent

sets of experiments. Frame size correlates to 35x35 μm . Error bars represent SEM. Significance levels are indicated.

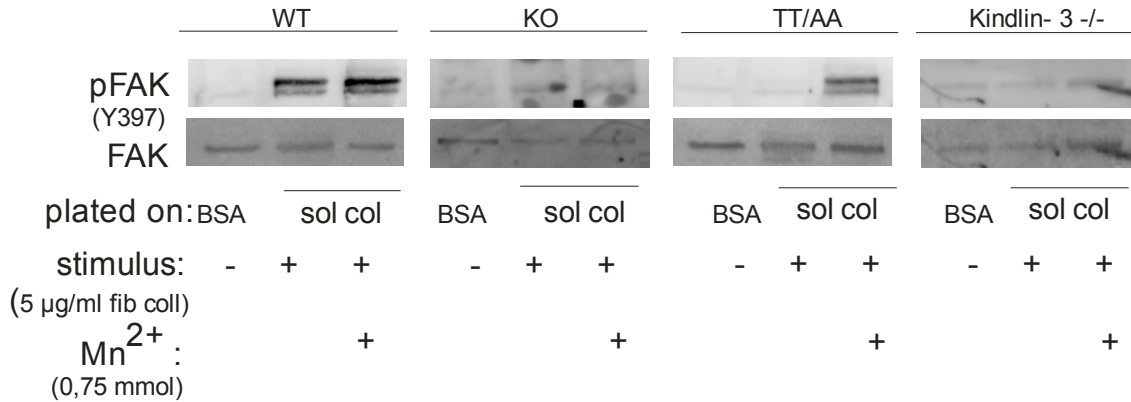


Figure 8: $\beta 1^{\text{TTAA/-}}$ platelets show a defective outside-in signaling and FAK phosphorylation which can be rescued by addition of manganese. Notably, the presence of kindlin-3 is required for FAK phosphorylation. Platelets (15×10^6 cells/ $150 \mu\text{l}$) were stimulated with $5 \mu\text{g/ml}$ fibrillar collagen and seeded on $25 \mu\text{g/ml}$ acid soluble collagen I (sol col) in the absence or the presence of $0.75 \text{ mmol Mn}^{2+}$. After 30min cells were immediately lysed in 1x laemmli buffer and subjected to immunoblotting for pFAK^{Y397}.

4.6 Tailbleeding assay

Being able to show a functional defect of $\beta 1^{\text{TTAA/-}}$ platelets ex vivo we wanted to address the in vivo relevance of our observations. To exclude side effects due to Mx1-Cre mediated $\beta 1$ integrin deletion in other organs (58, 72), all in vivo experiments were performed with bone marrow chimeras (Figure 3). Reduced $\beta 1$ integrin expression levels or the expression of mutant $\beta 1^{\text{TTAA}}$ integrins had no impact on thrombopoiesis as platelet counts were similar between all groups (Figure 9B). A former study suggested that deletion of $\beta 1$ integrins in blood cells did not result in an obvious bleeding defect (26). However, recently designed small molecule inhibitors, targeting $\alpha 2\beta 1$ integrin (73) conferred thrombosis protection in mice and supported previous findings by Sarrat et al. (29), which found prolonged tail bleeding times in $\alpha 2$ integrin deficient mice. By using a more sensitive and easier controllable tail bleeding assay (discussed below), we measured a significantly prolonged tail bleeding time in $\beta 1^{\text{TTAA}}$ mice, which was comparable to

$\beta 1$ deficient mice. Bleeding usually stops approximately after 8 to 9 min in both groups. Wild-type and heterozygous animals showed bleeding times between 2 to 3 min. Consistent with previous experiments, kindlin-3 deficient mice showed a severe bleeding phenotype due to an additional defect in $\alpha IIb\beta 3$ integrin activation (35). Notably, hypomorphic mice expressing only ~3% of the normal $\beta 1$ integrin levels showed normal bleeding times, indicating that very low amounts of active $\beta 1$ integrins are already sufficient to trigger hemostasis (Figure 9A).

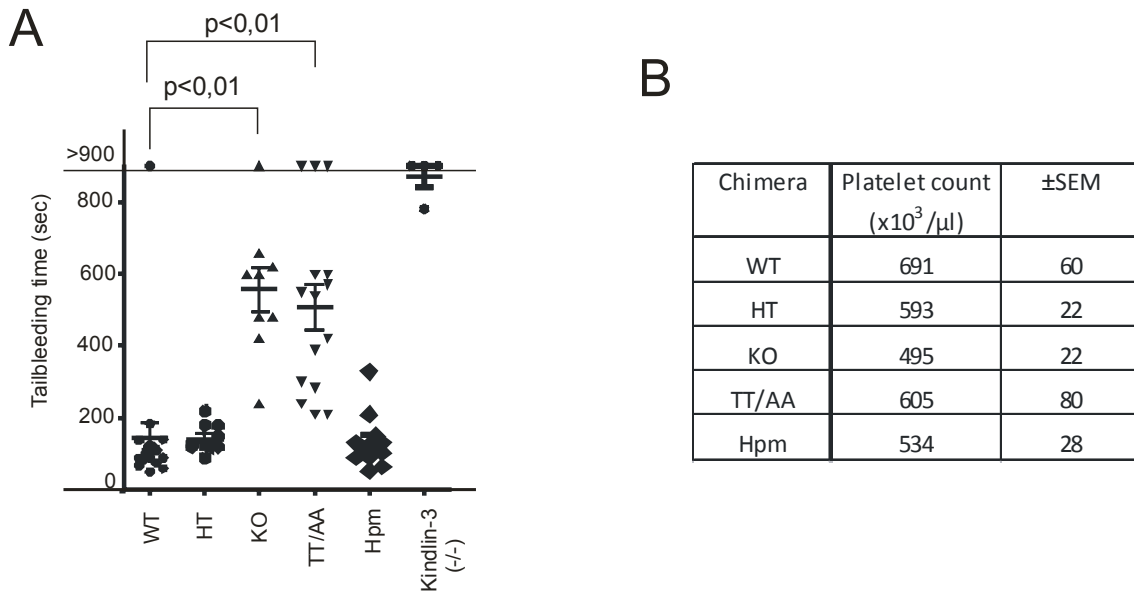


Figure 9: $\beta 1^{-/-}$ and $\beta 1^{TTAA/-}$ mice show prolonged bleeding times. (A) Tailtips of isoflurane narcotized animals were cut off. Tails were immediately placed into 37°C saline solution and time until bleeding stopped was measured (every symbol represents 1 animal). Tail bleeding exceeding 15 min was stopped by cauterization to prevent death. (B) Platelet counts were determined using Hemovet blood counter (WT (n=4), HT (n=3), KO (n=7), TT/AA (n=8), Hpm (n=8)). Mean bleeding times are indicated as bars, and error bars represent \pm SEM.

4.7 Carotid ligation assay

To analyze the role of $\beta 1$ integrins in platelet adhesion to wounded vessel walls in more detail, we performed *in vivo* carotis ligation assays. In this model, single platelet adhesion to a severe vessel wound (61) is monitored over time. In contrast to an earlier study, we found a significant reduction in adherent $\beta 1$ integrin deficient platelets at all time points (Figure 10). Beside $\beta 1$ integrin deficient platelets, $\beta 1^{\text{Hpm}/-}$ and $\beta 1^{\text{TTAA}/-}$ platelets showed a similar reduction in adhesion to the wounded vessel wall. This indicated that 18% $\beta 1^{\text{TTAA}}$ and 3% of $\beta 1$ integrin surface expression are not sufficient to mediate initial platelet adhesion.

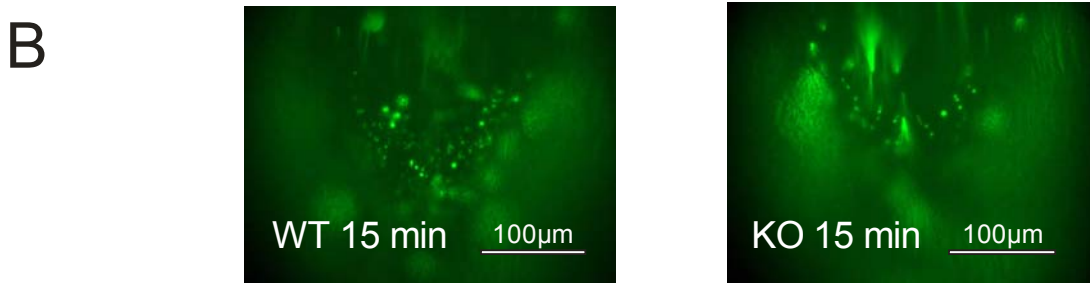
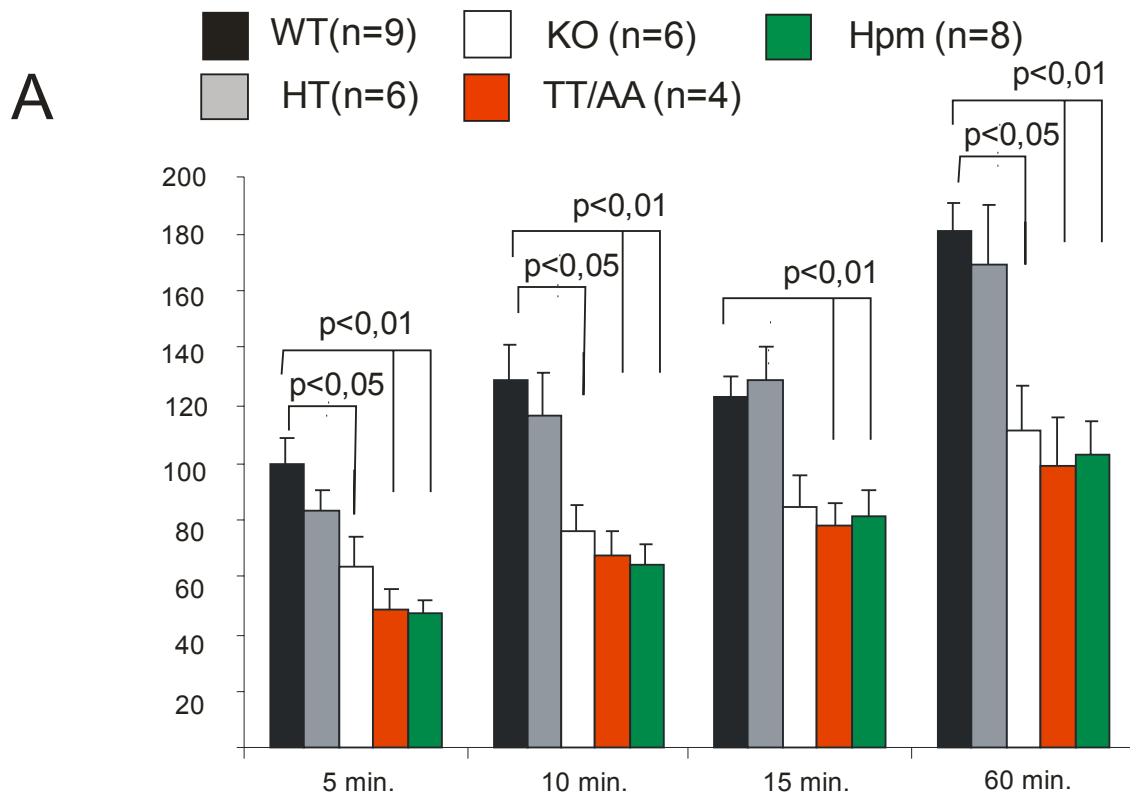


Figure 10: Single platelet adhesion analyzed in a carotid ligation model. $\beta 1^{-/-}$, $\beta 1^{TTAA/-}$, $\beta 1^{Hpm/-}$ mice show reduced single platelet adhesion to a vessel wound. Carotid arteries were ligated for 5 min and DCF labeled adherent platelets were counted after 5, 10, 15 and 60 min (A). Significance levels and animal number (n) per group are indicated. Platelet adhesion is shown in % (y-axis of cells adherent at 5 min time point in WT animals). (B) Representative pictures of 15 min time point of WT and KO animal are shown.

4.8 Aggregation assays

As in vivo data accentuated a signaling instead of the adhesive function of $\beta 1$ integrin in hemostasis, we decided to perform aggregation experiments using a light aggregometer. Convulxin a strong GPVI agonist induced similar aggregation in all tested platelet populations (Figure 11A, C). Stimulation with 5 $\mu\text{g/ml}$ fibrillar collagen, which binds GPVI and $\alpha 2\beta 1$ integrin leads to platelet aggregation in wild-type and heterozygous platelets. In strong contrast, $\beta 1$ deficient platelets failed to aggregate at all and $\beta 1^{TTAA/-}$ mutant platelets showed significantly reduced aggregation. Hypomorph platelets showed an intermediate phenotype (Figure 11A, B). To show that defective $\beta 1$ integrin activation and subsequent signaling in $\beta 1^{TTAA/-}$ platelets is responsible for the aggregation defect, $\beta 1^{TTAA/-}$ mutant platelets and $\beta 1^{-/-}$ platelets were incubated with fibrillar collagen in the presence of 0.75 mM Mn^{2+} . Indeed, bypassing $\beta 1$ integrin inside-out activation by Mn^{2+} rescued the aggregation defect in $\beta 1^{TTAA/-}$ mutant, but not in $\beta 1^{-/-}$ knockout platelets (Figure 12), indicating that signals arising from activated $\beta 1$ integrin are crucial for platelet aggregation. Furthermore, addition of fibrinogen into the reaction tube rescued the aggregation effect of $\beta 1^{+/TTAA}$ and $\beta 1^{-/-}$ platelets, suggesting that defective secretion of fibrinogen loaded vesicles might be responsible for the aggregation defect (Figure 12).

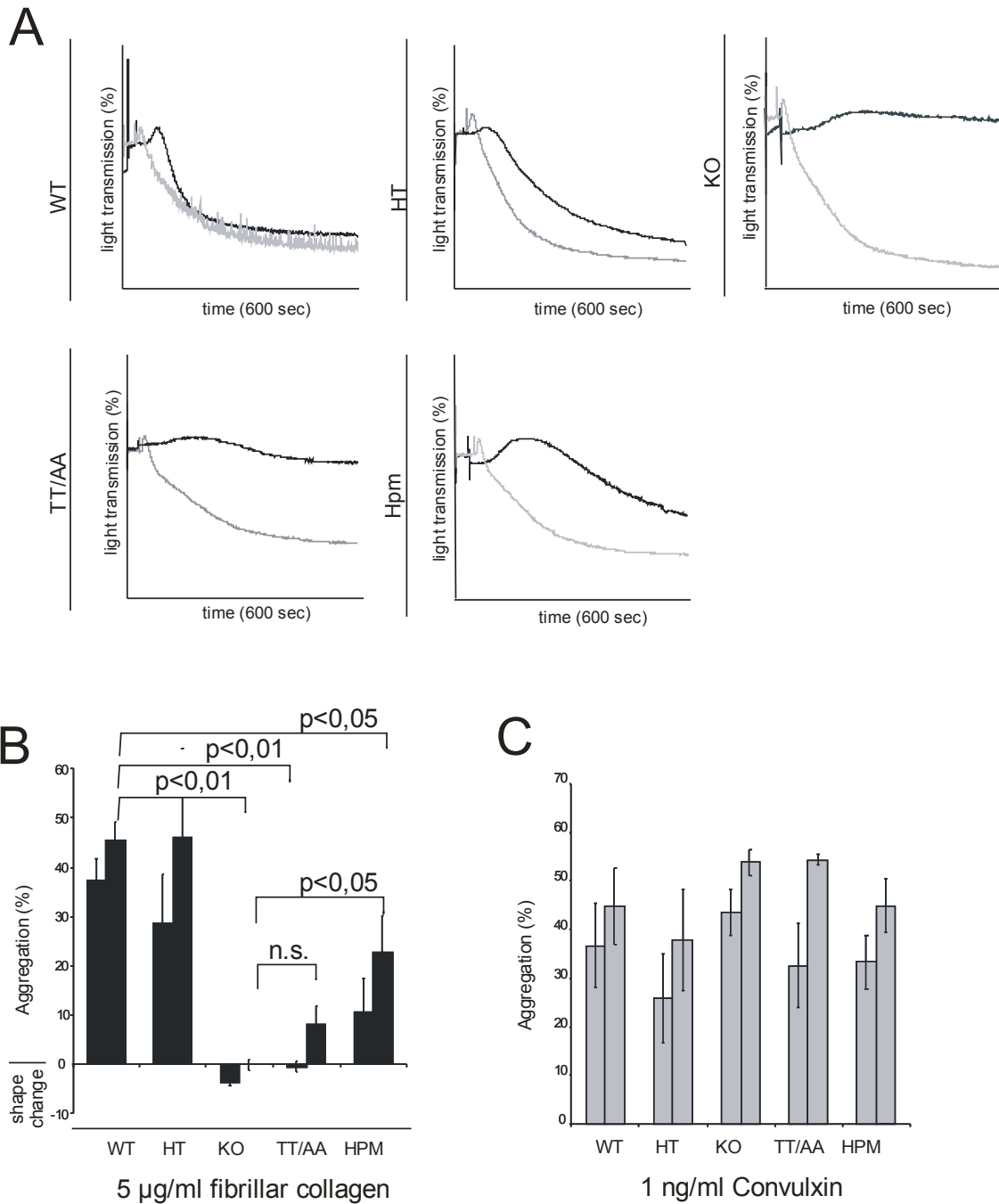


Figure 11: $\beta 1$ integrins are required for fibrillar collagen induced aggregation in vitro. (A) Platelets (1×10^8) were stimulated with 1 ng/ml convulxin (gray graphs) or 5 μ g/ml fibrillar collagen (black graphs) and aggregation was plotted for 600 sec $N \geq 4$ animals per group. Quantification of aggregation experiments after collagen (B) or convulxin stimulation (C) is shown. Two columns per group represent 300 sec and 600 sec time point. Significance levels are indicated. Error bars represent SEM.

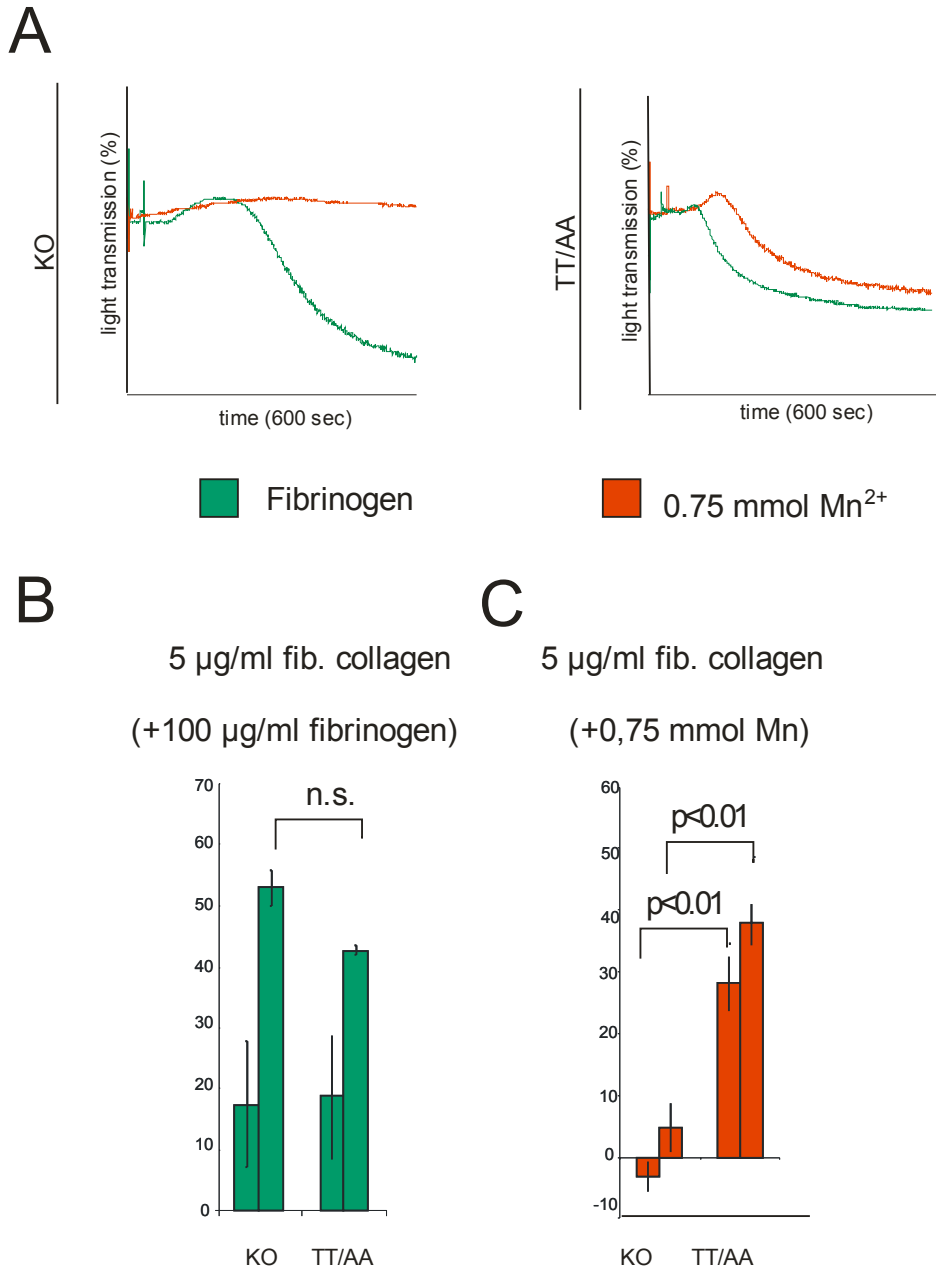
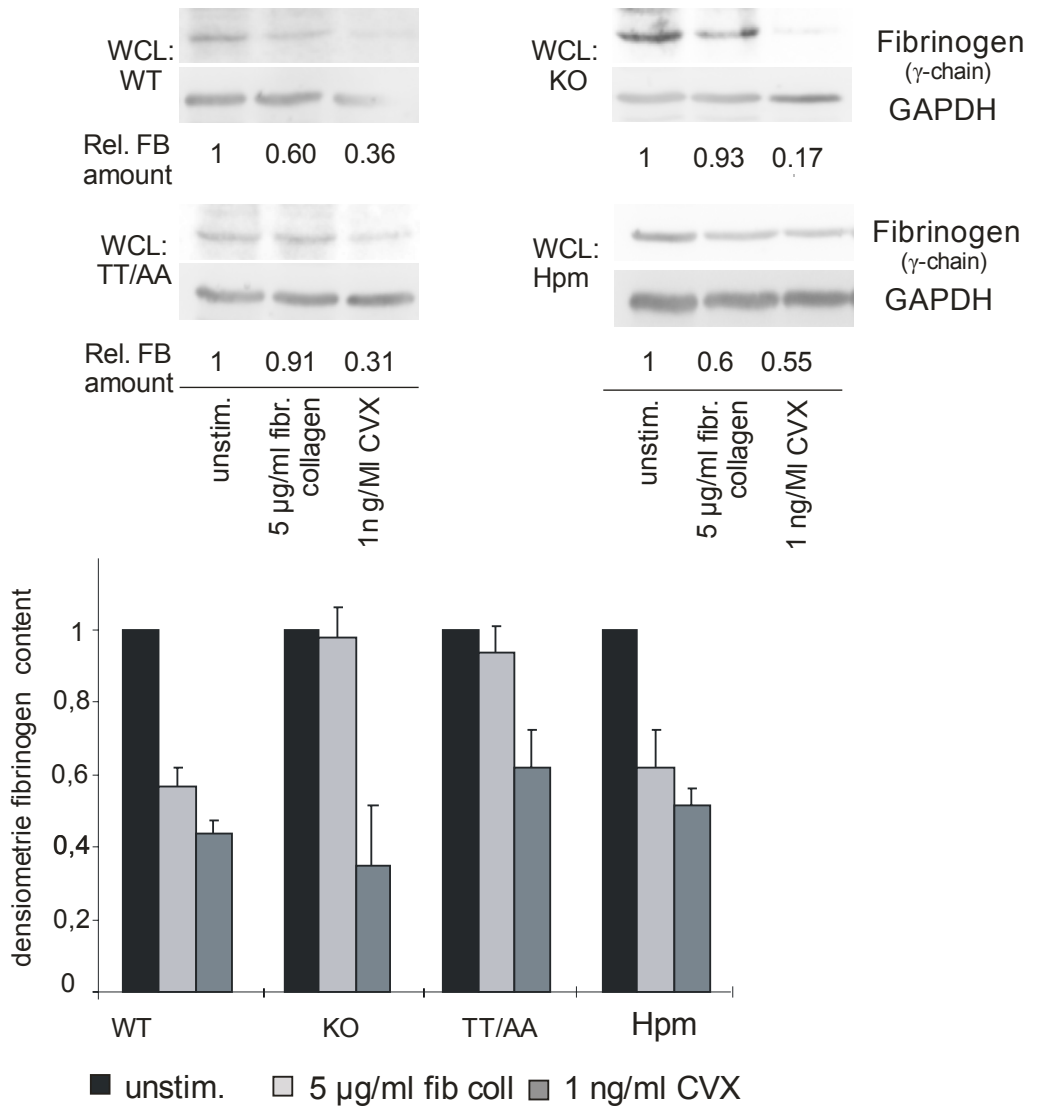


Figure 12: (A) Presence of fibrinogen or Mn²⁺ can rescue aggregation defect in $\beta 1^{TTAA/}$. Aggregation of fibrillar collagen stimulated platelets, in the presence of 100 $\mu\text{g/ml}$ fibrinogen or Mn²⁺ is shown. Depicted graphs are representative for $n \geq 3$ independent experiments per group. Quantification of aggregation experiments after collagen stimulation in the presence of fibrinogen (B) or manganese (C). Two columns per group represent 300 sec. and 600 sec. time points. Significance levels are indicated. Error bars represent SEM.

4.9 Dense granula and α -granula secretion

In line with earlier studies on $\alpha 2\beta 1$ deficient platelets (26, 74), we found a delayed maximal shape change in $\beta 1$ knockout ($t=144\pm 23$ sec, $n=6$) and $\beta 1^{TTAA/-}$ platelets ($t=143\pm 34$ sec, $n=5$) compared to wild-type ($t=35\pm 17$ sec, $n=4$) and heterozygous platelets ($t=44\pm 19$, $n=4$). Hypomorph platelets showed again an intermediate time ($t=94\pm 23$ sec, $n=5$). The initial shape change mainly depends on dense granule secretion, which releases different para- and endocrine agonists, such as ADP, ATP, GTP, GDP, serotonin, calcium, magnesium or 5-hydroxytryptamine that promote a positive feed forward loop. These mediators trigger an auto- and paracrine activation of platelets and subsequent aggregation and thrombus formation in vivo. To determine dense granule secretion we used a luciferase reporter system in a luminescence aggregometer. Platelets were stimulated either with 0.1 ng/ml convulxin or 5 μ g/ml fibrillar collagen. The collagen induced luminescence signal value and the convulxin signal value are represented as ratio (Figure 14). Interestingly, integrin deficient and mutant $\beta 1^{TTAA/-}$ platelets have a severe defect in dense granule secretion after fibrillar collagen stimulation. In parallel to dense granulas, platelets secrete numerous matrix molecules and other prothrombotic molecules stored in α - granules such as contain as fibrinogen, fibronectin, thrombospondin or vWF (75). Secretion from α -granule was indirectly determined by immunoblotting for cellular fibrinogen before and 8 min after agonist treatment (5 μ g/ml fibrillar collagen or 1 ng/ml CVX), under stirring conditions in an aggregometer. Convulxin stimulation induced a strong fibrinogen release with a reduction of the intracellular fibrinogen pool in platelets of all genotypes. On the contrary, fibrillar collagen induced fibrinogen release only in wild-type and hypomorphic platelets. $\beta 1^{-/-}$ knockout and $\beta 1^{TTAA/-}$ mutant platelets showed almost no decrease of the cellular fibrinogen content (Figure 13A, B). To rule out that the observed differences are due to reduced overall fibrinogen level, we blotted for total fibrinogen level (Figure 13C).

A



B

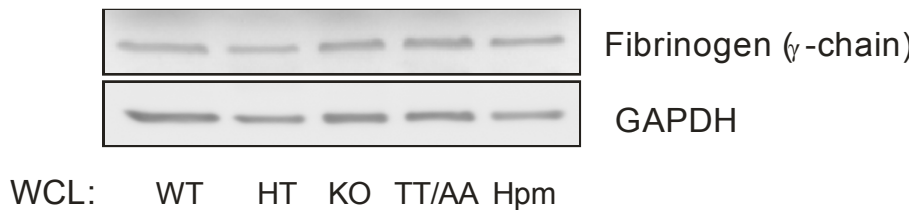


Figure 13: $\beta 1$ integrins are required for fibrinogen secretion after collagen stimulation. (A) Cells were stimulated for 8 min in an aggregometer with either 5 $\mu\text{g/ml}$ fibrillar collagen or 1 ng/ml convulxin (control). Next, cells were spun down and subjected to immunoblotting for fibrinogen (γ chain) and GAPDH as loading control. (B) No differences in cellular

fibrinogen loading in non-stimulated platelets is shown by immunoblotting of whole cell lysates for fibrinogen (γ -chain). GAPDH shows equal loading. Blots show one representative experiment.

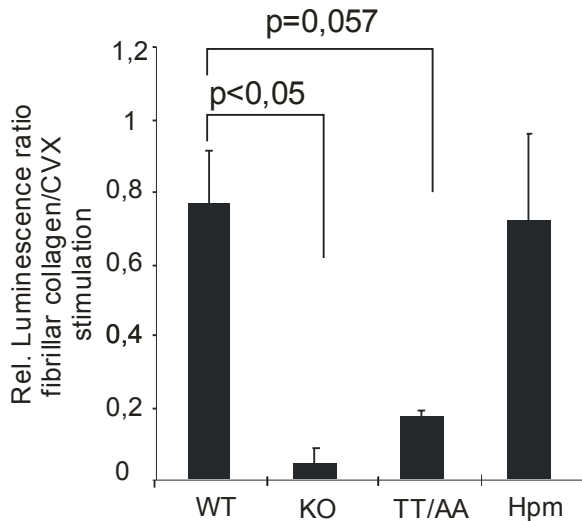


Figure 14: Dense granula secretion upon fibrillar collagen stimulation depends on $\beta 1$ integrins. Aggregation experiments (see above) were performed in the presence of a luciferin/luciferase reporter system to visualize ATP release from dense granula. Platelets were stimulated with either 5 $\mu\text{g/ml}$ fibrillar collagen or 1ng/ml convulxin. Detected luminescence (maximal signal strength) was expressed as ratio of fibrillar collagen stimulated to CVX stimulated cells. Bars represent mean values, error bars represents $\pm\text{SEM}$ of at least 3 independent experiments ($n \geq 3$). Significance levels are indicated.

4.10 Integrin tail phosphorylation

We showed that impaired kindlin-3 binding to double threonine mutated cytoplasmic tails has a physiological relevance. However, kindlin-3 binding might be also affect by phosphorylation within the tail. So far no phosphorylation of Thr 788 or 789 in platelets was reported. Hence, we wanted to know if both threonine residues can be phosphorylated in vivo and if so, can it be induced by platelet activation. Therefore, wild-type platelets were stimulated with 0.1 U/ml thrombin in the presence of 50 nmol Calyculin A and analyzed by non-quantitative mass spectrometry. We found peptides which correspond to $\beta 1$ integrin protein with both

threonine residues individually phosphorylated, however, we failed to detect double threonine phosphorylated peptides. A kinase-data base search predicted PKC as a potential kinase (NetPhosK 1.0: sequence: WDTGENPIYKSAVTTVVNPKYEGK, Thr788: score 0.70/1; Thr789: score 0.76/1) (Figure 15).

No.	Detected Peptide sequences	Predicted Kinase (likelihood score)
1	-WDTGENPIYK-	
2	-SAVTTVVNPK-	
3	-SAV(ph)TTVVNPK-	PKC (0.70/1)
4	-SAVT(ph)TVVNPk-	PKC (0.76/1)

Figures 15: β 1 integrins are phosphorylated in vivo, potentially by PKC family kinases. Lysates of thrombin stimulated platelets were separated on SDS gel, Coomassie stained and the corresponding bands of the approximate molecular weight of β 1 integrin were sent to mass spectrometry to analyze phosphorylation state of threonines 788/789. Table summarizes detected phosphopeptides after 60 seconds of thrombin stimulation of two independent experiments (n=2). Phospho-data base search (NetPhosK 1.0: sequence: WDTGENPIYKSAVTTVVNPKYEGK) predicted PKC family kinases as potential kinases (likelihood score: Thr788: 0.70/1; Thr789: 0.76/1).

5. Discussion

5.1 $\beta 1^{TTAA}$ integrins

Our former study showed that kindlin-3 is indispensable for integrin inside-out activation (35). We further showed that the kindlin binding site within the $\beta 1$ integrin cytoplasmic domain comprises a double threonine motif (TT788/789) which is located membrane proximal to the second NPxY motif, which is also required for kindlin binding. Since a recent study using recombinantly expressed $\alpha IIb\beta 3$ integrin which was reconstituted as single heterodimers within membrane discs showed a conformational switch from an inactive towards an active conformation in a talin dependent manner but in the absence of kindlin (39), it was questioned whether integrin inside-out signaling requires an integrin-kindlin interaction. Therefore, it was suggested that the phenotypes that are caused by kindlin deficiencies in man and various animal models are due to so far unknown cellular defects. To clarify these points, we analyzed $\beta 1$ integrin function in platelets of mice, in which the double threonine motif was mutated to two alanine residues. Using this approach we can clearly show that the kindlin-3 binding motif within the $\beta 1$ integrin cytoplasmic domain is indispensable for $\beta 1$ integrin inside-out activation and subsequent downstream signaling. Our data therefore disprove that talin-1 is sufficient to activate integrins. A likely explanation for this contrariety might be given by the fact that Shattil et al. (33) used an artificial in vitro setting neglecting the complexity and variety of other protein interactions at the integrin tail found in a living cell. In contrast, our data come from in-vivo experiments that encountered all physiological regulatory mechanisms.

5.1.1 $\beta 1^{TTAA}$ integrin outside-in signaling

During our study we further showed that kindlin-3 is required for integrin outside-in signaling. Integrin downstream signaling leads to the phosphorylation of signaling molecules such as Src, Syk, SLP-76, phospholipases and FAK (7, 76). Kindlin-3 null and $\beta 1^{TTAA/-}$ platelets fail to phosphorylate FAK upon collagen stimulation. Interestingly we found that addition of manganese that externally activates integrins, could rescue FAK phosphorylation and the spreading and aggregation defects in $\beta 1^{TTAA/-}$ platelets but failed to rescue FAK phosphorylation in kindlin-3

null platelets. Although the precise mechanism remains to be described, we provide evidence that FAK phosphorylation and integrin outside-in signaling require the presence of kindlin-3 but not a direct interaction between kindlin-3 and the integrin.

5.1.2 Integrin tail binding partner

A general limitation of our genetic animal model system remains that we cannot exclude that the $\beta 1^{\text{TAA}}$ mutation affects the binding of other integrin regulators, such as ILK, filamin A, or 14-3-3 protein, since their binding sites overlap with the kindlin binding site (77). However, these proteins are not involved in integrin inside-out signaling, but rather play a role in outside-in signaling. For example, ILK null platelets show only slightly decreased $\alpha \text{IIb}\beta 3$ integrin activation quantified by fibrinogen binding, whereas α -granula secretion and aggregation upon collagen stimulation were severely impaired (78). In our preliminary pulldown experiments we measured (data not shown) only a slight reduction of ILK binding to the $\beta 1^{\text{TAA}}$ cytoplasmic tail, arguing that threonines 788/789 are not essential for the ILK binding. However, future experiments should use a proteome wide approach to search for all known candidate interactors as well as unknown ones. A quantitative mass spectrometry would offer a sophisticated and elegant way to address this question. The SILAC (Stable isotope labeling with amino acids in cell culture) approach uses cell lysates from mice which were fed with a diet that only contained a $^{13}\text{C}^{(6)}$ -isotope substituted lysine (referred as “heavy lysate”) (79) which can be distinguished from “non-heavy lysates” by mass spectrometry. Using lysates from SILAC mice versus non-SILAC mice will allow the calculation of protein binding ratios. A technical limitation of this approach arises from contaminations of unspecific bound proteins within pulldown eluates. Peptides used for pulldown experiments by us and others in earlier studies (35, 38) facilitated a hexa-histidine tag which was bound by nickel loaded agarose beads. Highly positively charged nickel beads exhibit a high degree of molecular stickiness and subsequent unspecific background protein binding. We therefore redesigned the integrin tails in a way that we could use a biotin streptavidin-bead system to pullout integrin tails. By this tool, we hope to decrease background binding within future mass spectrometry experiments.

5.1.3 Threonine phosphorylation of the integrin tail

Another mechanism might as well contribute to reduced kindlin-3 binding to $\beta 1^{\text{TTAA}}$ integrin. Replacing two potential phosphorylation sites could impair regulatory mechanism which control protein interactions at the tail. Protein phosphorylation is a fast and efficient way to rapidly change protein charges and binding affinities. Several so called phospho-switches by site directed phosphorylation at the integrin tail are described (77). Our data showed for the first time that both Thr 788 and Thr 789 residues are phosphorylated, although not simultaneously. However, phosphorylation was only found in the presence of the Serine/Threonine phosphatase inhibitor calinculyn A (80), arguing that only a minor pool of $\beta 1$ integrins is phosphorylated. Experimental evidence for a threonine phospho-switch within the integrin tail comes from studies in T cells. Phosphorylation of Thr 758 (corresponding to the proximal Thr 788) in $\beta 2$ integrin regulates Filamin-A and protein 14-3-3 binding to the cytoplasmic tail. Thereby, filamin-1 binds to the unphosphorylated $\beta 2$ integrin subunit, but falls off from phospho Thr 758 allowing 14-3-3 binding (81), followed by increased cell spreading and migration (77). Another study showed that inhibition of Serine/Threonine phosphatases leads to a more sustained $\beta 3$ integrin activation, likely through integrin phosphorylation (82). It is tempting to speculate that a similar phospho-switch mechanism regulates kindlin-3 binding to the tail and thereby inside-out activation of $\beta 1$ integrins. A kinase data base search predicted PKC to be the potential kinase, responsible for Thr 788/ 789 phosphorylation although with a low likelihood score of around 0.7. In line with our hypothesis, a recent study showed that PKC α deficient platelets have defect $\beta 3$ inside-out activation, granula secretion and reduced thrombus formation in vivo (83). Drawing another analogy to talin-1 reveals a similar phospho-switch mechanism for tail binding (34). Phosphorylation at the proximal NPxY motif of $\beta 3$ integrins differentially regulates tail binding of talin-1 and tensin-1, an actin crosslinker protein. Interestingly talin binding is negatively regulated by phosphorylation and talin gets displaced from phospho-tyrosine residues enabling tensin to bind and to increase adhesion strength. In summary, our data support the hypothesis that kindlin-3 binding to the cytoplasmic tail is regulated by a threonine phospho-switch. Therefore, further experiments analyzing kindlin affinity to a differently phosphorylated tail are required to validate our hypothesis.

5.1.4 $\beta 1^{\text{TAA}}$ expression level

To our surprise, the introduction of the kindlin-binding site mutation into the $\beta 1$ integrin results in a strong reduction of $\beta 1$ integrin expression in platelets. We previously showed that kindlin-3 deficient platelets have reduced $\beta 1$ integrin surface levels (35) suggesting that an interaction between kindlin-3 and the cytoplasmic domain of the $\beta 1$ integrin is required for normal $\beta 1$ integrin expression. A similar observation was made in $\beta 3$ integrin mutant mice, which lack the last three c-terminal residues (RGT) (84). Although the RGT residues are directly adjacent to the membrane distal NPXY motif, it remains speculative whether kindlin binding is affected by this deletion. The molecular cause for these observations is still unclear and requires further investigations.

5.2 $\beta 1$ integrins in arterial thrombosis

Various groups analyzed platelet $\beta 1$ integrin contribution in hemostasis in animal models. However, the acquired data and conclusions remain inconsistent. Analyzing our two newly generated mouse models ($\beta 1^{\text{TAA}/-}$ MxCre, $\beta 1^{\text{Hpm}/-}$ MxCre), we clearly show that $\beta 1$ -integrins facilitate an important signaling role in- and ex-vivo by regulating platelet granula secretion, aggregation and thrombus formation. Unexpectedly, we find that collagen signaling by GPVI is insufficient to activate platelets and requires an additional $\beta 1$ integrin mediated signal. Furthermore, we could show that $\beta 1$ integrins contribute to single platelet adhesion in vivo. A possible explanation for different results might arise from different experimental settings (discussed below) as well as different animal models, namely $\beta 1$ integrin depleted versus $\alpha 2\beta 1$ depleted platelets, being used. Hence a careful review of experimental setups might give reasonable explanation.

Regarding clinical implications, our data underline the therapeutic potential of $\beta 1$ integrin inhibition during treatment of acute arterial thrombosis. Although an obvious limitation might be that inhibitor molecules would have to reach 100% receptor blockade with a sufficient pharmacokinetics, as $\sim 3\%$ of intact integrin are sufficient to reach full platelet activation upon collagen stimulation.

5.2.1 Bone marrow chimera

Bone marrow chimeras are an elegant way to avoid off-target conditional gene deletion in vivo. It was shown that poly I:C induced expression of Cre-recombinase efficiently deletes the conditional gene loci in the hematopoietic system and some other off-target tissues including kidney or liver cells (58). Preliminary experiments showed that poly I:C treated $\beta 1^{-/-}$ MxCre animals have a severe and sustained liver failure with a strong inflammatory phenotype and a confined liver synthesis capacity (Petzold et al. unpublished). This phenotype is not seen in bone marrow chimeras carrying a $\beta 1^{-/-}$ MxCre bone marrow in a C57/BL6 mouse background. As an altered liver synthesis might affect plasma proteins level and by this platelet granular content of internalized plasma proteins which get released upon platelet activation (85). In summary, generation of bone marrow chimeras is essential to prevent off-target effects.

5.2.2 Carotid ligation assay and occlusive thrombus formation

Keeping in mind that $\beta 1$ integrin expression levels (e.g. approximately 3000 $\alpha 2\beta 1$ integrins per cell) are minor compared to $\beta 3$ integrin levels (e.g. approximately 60000 receptors per cells), it seems critical to find experimental conditions that are sensitive enough to uncover $\beta 1$ specific function. First, we analyzed single platelet adhesion in a carotid ligation model. Our results clearly show that $\beta 1$ integrins play a significant role in single platelet adhesion in vivo. The reason for the impaired adhesion of $\beta 1^{\text{TTAA}/-}$ mutant platelets is hard to interpret since we found an integrin activation defect and reduced $\beta 1^{\text{TTAA}}$ integrin surface expression. An appropriate control animal with around 18% functional integrin $\beta 1$ is needed to allow conclusions on the importance of $\beta 1^{\text{TTAA}}$ integrin in this process.

Our findings contradict the data generated by Gruner et al. (27), who found no adhesion defect in the same $\beta 1^{-/-}$ MxCre animals and the same thrombosis model. A possible reason for the discrepancy might be that this group did not use bone-marrow chimeras (see above). Furthermore, they found occlusive thrombus formation in WT animals which was neither seen by us nor by Massberg et al. (61). Electron microscopic images from ligation areas by Massberg et al. revealed a well defined arterial lesion with endothelial cell denudation and matrix exposure after 5 min of vessel occlusion. In contrast, Gruner et al. used a ligation time of

only 30 sec without a precise description of their induced lesion. It is likely that other thrombosis inducing mechanisms (e.g. tissue factor) overweight the contribution of platelet-matrix interaction as primary stimulus.

Second, we wanted to analyse the role of $\beta 1$ integrins in occlusive thrombus formation. Several models are applicable to induce an occlusive arterial thrombosis in mice (61, 86) and various were used to study $\beta 1$ -integrin contribution. He et al. (30) found prolonged vessel occlusion times in a photochemical assay but no $\beta 1$ -integrin contribution in a pulmonary embolism model (86). The photochemical injury model is based on increased reactive oxygen production within the endothelium and potentially other less well defined mechanism (86). Hence a limitation of the model remains that it might be unsuitable to study ECM induced thrombosis. Kuijper used a Ferric-(III)-chloride model in integrin $\alpha 2$ null animals and found no difference in thrombus formation but decreased thrombus stability with frequently appearing embolic events in these animals (87). However, the underlying thrombosis inducing mechanism was shown to (mainly) rely on increased thrombin generation on the surfaces of ferric ion filled particles exposed on the endothelium and the exposed matrix shortly after placement of an Ferric chloride soaked paper on mesenteric arteries (88). This thrombosis model was shown to be insensitive to GPVI or $\beta 1$ depletion and might therefore lead to an underestimation of $\beta 1$ contribution in vivo. Trying to find a reasonable model to analyze (primarily) extra cellular matrix induced thrombosis, we decided to perform tailbleeding assays. Historically, bleeding assays were developed to screen for bleeding disorders in patients. For animal studies two different protocols were established in analogy to the clinical tests by Marx or Ivy. We decide to adapt the protocol by Marx to measure tail bleeding times. Therefore, tail tips of chimera animals were cut and placed into an isotonic 37°C warm water bath and time till bleeding stopped was measured. As a high degree of reproducibility and standardization is needed to reveal minor bleeding phenotypes, as expected for $\beta 1$ integrin null animals, we set our wound 8 mm away from tail tips in 10-12 weeks old chimeras. Further, we choose an isofluran gas narcosis instead of intraperitoneal application of drugs (26, 89). This technique allowed a steady narcosis depth, monitored by breathing frequency, to prevent massive changes within circulatory parameters. Obviously, anatomical alteration of the tail vasculature between individual mice might lead to some variation in

bleeding behavior. Surprisingly, we found that as little as ~3% of functional $\beta 1$ integrins found in hypomorph mice are sufficient to yield normal bleeding and vessel occlusion times. In contrast $\beta 1$ integrin null mice or inactive integrin $\beta 1^{\text{TT/AA}}$ carrying mice showed prolonged bleeding times. Our results are in line with other studies using $\alpha 2\beta 1$ depleted animals (29-30), but contradict two others (26, 89). The later used a bleeding assays adapted from clinical setting by Ivy, in which blood drops at the lesion were removed by whatman paper every 30 seconds until bleeding stopped. We tried to reproduce our data by this assay, however found big variations even inside the control group (preliminary data, not shown), as manipulating on the tail often caused disclosure of the lesion or sometimes an immediate bleeding arrest. In summary, our in vivo data show an important role of $\beta 1$ integrins for platelet adhesion and occlusive thrombus formation.

5.2.3 Aggregation and secretion

Trying to find a mechanism which might help to explain our tailbleeding data, we studied platelet aggregation. Earlier aggregation assays on $\beta 1$ or $\alpha 2\beta 1$ integrin deficient platelets were performed in the presence of 100 $\mu\text{g/ml}$ fibrinogen and did not find any aggregation defect upon fibrillar collagen stimulation (26, 89). Interestingly, mouse fibrinogen plasma level in C57/BL6 mice range around 1.5 mg/ml and are therefore 15 times higher than used in above mentioned studies (90). As mimicking in vivo plasma conditions ex- vivo remains challenging, we performed our aggregation assays in the absence of fibrinogen or other plasma proteins and found an aggregation defect for $\beta 1$ null and $\beta 1^{\text{TTAA-}}$ platelets. Moreover, addition of MnCl_2 to $\beta 1^{\text{TTAA-}}$ platelets rescued the aggregation defect and underlined that $\beta 1$ derived signals are rather essential than just supportive as discussed above (91). Most surprisingly, we found that already minor amounts (~3%) of active $\beta 1$ integrins are sufficient to trigger integrin outside-in signaling and subsequent aggregation. We further could show that the aggregation defect is due to an inhibited dense (ATP) and fibrinogen secretion from α -granula. So far, GPVI was thought to overtake all collagen signaling in vivo, leading to platelet activation, aggregation and granular secretion (26, 61-62, 92). However, earlier work from Chen et al. (91) suggested a two side two-step model in which $\alpha 2\beta 1$ activation is downstream of GPVI and generates similar signals that merge into

GPVI downstream signaling pathways via Syk, SLP-76. These authors limited their hypothesis to conditions in which $\alpha 2\beta 1$ signaling might compensate for insufficient GPVI signaling (e.g. in the presence of GPVI blocking reagents). We show that $\beta 1$ integrin signaling is required and indispensable for granula release and subsequent aggregation even in the presence of high concentrations (5 μ g/ml) of fibrillar collagen (93). Future studies have to address the precise molecular signaling pathways how $\beta 1$ integrin signaling affect granular secretion.

6. Summary

The affinity state of integrins is regulated by two cytoplasmic integrin binding proteins: talin and kindlin. Loss of either of them results in inactive integrins in various cell types. To test whether a direct interaction between kindlin and the integrin is required for integrin activation (integrin inside-out signaling) and $\beta 1$ integrin mediated signaling (integrin outside-in signaling) we analyzed platelets from mice expressing a kindlin-binding deficient $\beta 1$ integrin ($\beta 1^{\text{TTAA}}$). Our data clearly show that integrin inside-out signaling depends on a direct integrin-kindlin interaction as $\beta 1^{\text{TTAA}}$ integrins remain inactive upon platelet activation by soluble agonists. On the contrary, exogenous activation of $\beta 1^{\text{TTAA}/-}$ platelets by manganese results in normal cell spreading and FAK phosphorylation indicating that outside-in signaling does not depend on a direct interaction. Furthermore, mice expressing $\beta 1^{\text{TTAA}}$ mutant integrins show prolonged bleeding times comparable to mice exhibiting a blood cell specific deletion of the $\beta 1$ gene. Single platelet adhesion to injured vessel walls is strongly reduced in $\beta 1$ null and $\beta 1^{\text{TTAA}}$ platelets suggesting an important role of $\beta 1$ integrins for initial platelet adhesion. In line with this observation, we show that $\beta 1$ integrin-mediated signals direct granula secretion, required for a pro-thrombogenic micro milieu favoring platelet adhesion and aggregation during the early phases of hemostasis. Most surprisingly, 3% of active $\beta 1$ integrin are sufficient to rescue bleeding defects.

7. Zusammenfassung

Die Aktivität von Integrinen wird durch die beiden zytoplasmatischen Proteine Talin und Kindlin reguliert. Der Verlust eines von beiden führt zu inaktiven Integrinen in verschiedenen Zelltypen. Um zu prüfen, ob eine direkte Integrin-Kindlin Interaktion für die Integrinaktivierung als auch die anschließende Signalgenerierung benötigt wird, haben wir die Funktion von Mausthrombozyten analysiert, deren $\beta 1$ Integrine nicht mehr in der Lage sind, Kindlin zu binden. Unsere Daten zeigen, dass für die Integrinaktivierung eine direkte Kindlin-Integrin Interaktion notwendig ist, da mutierte $\beta 1^{\text{TTAA}}$ Integrine nach Stimulation mit löslichen Agonisten inaktiv bleiben. Im Gegensatz dazu, findet sich nach externer Aktivierung der $\beta 1^{\text{TTAA}}$ Integrine durch Mangan ein normales Zellspreading sowie eine normale FAK Phosphorylierung. Diese Beobachtung zeigt, dass Integrin vermittelte Signale keine direkte Interaktion von Kindlin mit dem Integrin benötigen. Weiterhin haben Mäuse, deren Thrombozyten $\beta 1^{\text{TTAA}}$ Integrine exprimieren, verlängerte Blutungszeiten, die vergleichbar mit denen von $\beta 1$ Integrin (Blutzell-) depletierten Tieren sind. Die Anzahl adhärenter Thrombozyten an eine Gefäßläsion der Arteria carotis ist in $\beta 1$ -Integrin depletierten und $\beta 1^{\text{TTAA}}$ exprimierenden Tieren reduziert, was die wichtige Rolle der $\beta 1$ Integrine während der initialen Phase der Thrombozytenadhäsion hervorhebt. Weiterhin zeigen wir, dass $\beta 1$ vermittelte Signale die Granulasekretion steuern, die zur Schaffung eines pro-thrombotischen Mikromilieus notwendig ist, um somit eine weitere Thrombozytenadhäsion und Aggregation während der frühen Phase der Blutstillung zu unterstützen. Überraschenderweise reichen bereits ~3% an aktiven $\beta 1$ Integrinen auf den Thrombozyten, um eine normale Blutungszeit im Tiermodell zu erhalten.

References

1. Junt T, Schulze H, Chen Z, Massberg S, Goerge T, Krueger A, et al. Dynamic visualization of thrombopoiesis within bone marrow. *Science*. 2007;317(5845):1767-70.
2. Davi G, Patrono C. Platelet activation and atherothrombosis. *N Engl J Med*. 2007;357(24):2482-94.
3. Reininger AJ. Function of von Willebrand factor in haemostasis and thrombosis. *Haemophilia*. 2008;14 Suppl 5:11-26.
4. Massberg S, Brand K, Gruner S, Page S, Muller E, Muller I, et al. A critical role of platelet adhesion in the initiation of atherosclerotic lesion formation. *J Exp Med*. 2002;196(7):887-96. PMID: 2194025.
5. Tsuji M, Ezumi Y, Arai M, Takayama H. A novel association of Fc receptor gamma-chain with glycoprotein VI and their co-expression as a collagen receptor in human platelets. *J Biol Chem*. 1997;272(38):23528-31.
6. Li Z, Delaney MK, O'Brien KA, Du X. Signaling during platelet adhesion and activation. *Arterioscler Thromb Vasc Biol*. 2010;30(12):2341-9.
7. Varga-Szabo D, Pleines I, Nieswandt B. Cell adhesion mechanisms in platelets. *Arterioscler Thromb Vasc Biol*. 2008;28(3):403-12.
8. Nieswandt B, Varga-Szabo D, Elvers M. Integrins in platelet activation. *J Thromb Haemost*. 2009;7 Suppl 1:206-9.
9. Hynes RO. Integrins: bidirectional, allosteric signaling machines. *Cell*. 2002;110(6):673-87.
10. Cosemans JM, Iserbyt BF, Deckmyn H, Heemskerk JW. Multiple ways to switch platelet integrins on and off. *J Thromb Haemost*. 2008;6(8):1253-61.
11. Parsons JT, Horwitz AR, Schwartz MA. Cell adhesion: integrating cytoskeletal dynamics and cellular tension. *Nat Rev Mol Cell Biol*. 2010;11(9):633-43. PMID: 2992881.
12. Schwartz MA. Remembrance of dead cells past: discovering that the extracellular matrix is a cell survival factor. *Mol Biol Cell*. 2010;21(4):499-500. PMID: 2820415.
13. Fassler R, Meyer M. Consequences of lack of beta 1 integrin gene expression in mice. *Genes Dev*. 1995;9(15):1896-908.
14. Orr AW, Helmke BP, Blackman BR, Schwartz MA. Mechanisms of mechanotransduction. *Dev Cell*. 2006;10(1):11-20.
15. Schwartz MA. Integrins and extracellular matrix in mechanotransduction. *Cold Spring Harb Perspect Biol*. 2010;2(12):a005066.
16. Tzima E, Irani-Tehrani M, Kiosses WB, Dejana E, Schultz DA, Engelhardt B, et al. A mechanosensory complex that mediates the endothelial cell response to fluid shear stress. *Nature*. 2005;437(7057):426-31.
17. Orr AW, Sanders JM, Bevard M, Coleman E, Sarembock IJ, Schwartz MA. The subendothelial extracellular matrix modulates NF-kappaB activation by flow: a potential role in atherosclerosis. *J Cell Biol*. 2005;169(1):191-202. PMID: 2171897.
18. Zaidel-Bar R, Itzkovitz S, Ma'ayan A, Iyengar R, Geiger B. Functional atlas of the integrin adhesome. *Nat Cell Biol*. 2007;9(8):858-67. PMID: 2735470.
19. Zaidel-Bar R, Geiger B. The switchable integrin adhesome. *J Cell Sci*. 2010;123(Pt 9):1385-8. PMID: 2858016.
20. Bennett JS, Berger BW, Billings PC. The structure and function of platelet integrins. *J Thromb Haemost*. 2009;7 Suppl 1:200-5.
21. Kiefer TL, Becker RC. Inhibitors of platelet adhesion. *Circulation*. 2009;120(24):2488-95.
22. Nurden AT. Glanzmann thrombasthenia. *Orphanet J Rare Dis*. 2006;1:10. PMID: 1475837.
23. Hodivala-Dilke KM, McHugh KP, Tsakiris DA, Rayburn H, Crowley D, Ullman-Cullere M, et al. Beta3-integrin-deficient mice are a model for Glanzmann thrombasthenia showing placental defects and reduced survival. *J Clin Invest*. 1999;103(2):229-38. PMID: 407888.

24. Smyth SS, Reis ED, Vaananen H, Zhang W, Collier BS. Variable protection of beta 3-integrin--deficient mice from thrombosis initiated by different mechanisms. *Blood*. 2001;98(4):1055-62.
25. Bennett JS, Chan C, Vilaire G, Mousa SA, DeGrado WF. Agonist-activated alphavbeta3 on platelets and lymphocytes binds to the matrix protein osteopontin. *J Biol Chem*. 1997;272(13):8137-40.
26. Nieswandt B, Brakebusch C, Bergmeier W, Schulte V, Bouvard D, Mokhtari-Nejad R, et al. Glycoprotein VI but not alpha2beta1 integrin is essential for platelet interaction with collagen. *EMBO J*. 2001;20(9):2120-30. PMID: 125246.
27. Gruner S, Prostredna M, Schulte V, Krieg T, Eckes B, Brakebusch C, et al. Multiple integrin-ligand interactions synergize in shear-resistant platelet adhesion at sites of arterial injury in vivo. *Blood*. 2003;102(12):4021-7.
28. Kuijpers MJ, Schulte V, Bergmeier W, Lindhout T, Brakebusch C, Offermanns S, et al. Complementary roles of glycoprotein VI and alpha2beta1 integrin in collagen-induced thrombus formation in flowing whole blood ex vivo. *FASEB J*. 2003;17(6):685-7.
29. Sarratt KL, Chen H, Zutter MM, Santoro SA, Hammer DA, Kahn ML. GPVI and alpha2beta1 play independent critical roles during platelet adhesion and aggregate formation to collagen under flow. *Blood*. 2005;106(4):1268-77. PMID: 1895202.
30. He L, Pappan LK, Grenache DG, Li Z, Tollefsen DM, Santoro SA, et al. The contributions of the alpha 2 beta 1 integrin to vascular thrombosis in vivo. *Blood*. 2003;102(10):3652-7.
31. Penz S, Reininger AJ, Brandl R, Goyal P, Rabie T, Bernlochner I, et al. Human atheromatous plaques stimulate thrombus formation by activating platelet glycoprotein VI. *FASEB J*. 2005;19(8):898-909.
32. Pugh N, Simpson AM, Smethurst PA, de Groot PG, Raynal N, Farndale RW. Synergism between platelet collagen receptors defined using receptor-specific collagen-mimetic peptide substrata in flowing blood. *Blood*. 2010;115(24):5069-79. PMID: 2890152.
33. Shattil SJ, Kim C, Ginsberg MH. The final steps of integrin activation: the end game. *Nat Rev Mol Cell Biol*. 2010;11(4):288-300.
34. Moser M, Legate KR, Zent R, Fassler R. The tail of integrins, talin, and kindlins. *Science*. 2009;324(5929):895-9.
35. Moser M, Nieswandt B, Ussar S, Pozgajova M, Fassler R. Kindlin-3 is essential for integrin activation and platelet aggregation. *Nat Med*. 2008;14(3):325-30.
36. Nieswandt B, Moser M, Pleines I, Varga-Szabo D, Monkley S, Critchley D, et al. Loss of talin1 in platelets abrogates integrin activation, platelet aggregation, and thrombus formation in vitro and in vivo. *J Exp Med*. 2007;204(13):3113-8. PMID: 2150972.
37. Petrich BG, Fogelstrand P, Partridge AW, Yousefi N, Ablooglu AJ, Shattil SJ, et al. The antithrombotic potential of selective blockade of talin-dependent integrin alpha IIb beta 3 (platelet GPIIb-IIIa) activation. *J Clin Invest*. 2007;117(8):2250-9. PMID: 1906732.
38. Harburger DS, Bouaouina M, Calderwood DA. Kindlin-1 and -2 directly bind the C-terminal region of beta integrin cytoplasmic tails and exert integrin-specific activation effects. *J Biol Chem*. 2009;284(17):11485-97. PMID: 2670154.
39. Ye F, Hu G, Taylor D, Ratnikov B, Bobkov AA, McLean MA, et al. Recreation of the terminal events in physiological integrin activation. *J Cell Biol*. 2010;188(1):157-73. PMID: 2812850.
40. Crittenden JR, Bergmeier W, Zhang Y, Piffath CL, Liang Y, Wagner DD, et al. CalDAG-GEFI integrates signaling for platelet aggregation and thrombus formation. *Nat Med*. 2004;10(9):982-6.
41. Chrzanowska-Wodnicka M, Smyth SS, Schoenwaelder SM, Fischer TH, White GC, 2nd. Rap1b is required for normal platelet function and hemostasis in mice. *J Clin Invest*. 2005;115(3):680-7. PMID: 546455.
42. Cifuni SM, Wagner DD, Bergmeier W. CalDAG-GEFI and protein kinase C represent alternative pathways leading to activation of integrin alphallbbeta3 in platelets. *Blood*. 2008;112(5):1696-703. PMID: 2518880.

43. Han J, Lim CJ, Watanabe N, Soriani A, Ratnikov B, Calderwood DA, et al. Reconstructing and deconstructing agonist-induced activation of integrin alphaIIb beta3. *Curr Biol*. 2006;16(18):1796-806.
44. Hughes PE, Diaz-Gonzalez F, Leong L, Wu C, McDonald JA, Shattil SJ, et al. Breaking the integrin hinge. A defined structural constraint regulates integrin signaling. *J Biol Chem*. 1996;271(12):6571-4.
45. Wegener KL, Partridge AW, Han J, Pickford AR, Liddington RC, Ginsberg MH, et al. Structural basis of integrin activation by talin. *Cell*. 2007;128(1):171-82.
46. Vinogradova O, Haas T, Plow EF, Qin J. A structural basis for integrin activation by the cytoplasmic tail of the alpha IIb-subunit. *Proc Natl Acad Sci U S A*. 2000;97(4):1450-5. PMID: 26454.
47. Takagi J, Petre BM, Walz T, Springer TA. Global conformational rearrangements in integrin extracellular domains in outside-in and inside-out signaling. *Cell*. 2002;110(5):599-11.
48. Takagi J, Erickson HP, Springer TA. C-terminal opening mimics 'inside-out' activation of integrin alpha5beta1. *Nat Struct Biol*. 2001;8(5):412-6.
49. Moser M, Bauer M, Schmid S, Ruppert R, Schmidt S, Sixt M, et al. Kindlin-3 is required for beta2 integrin-mediated leukocyte adhesion to endothelial cells. *Nat Med*. 2009;15(3):300-5.
50. Kunicki TJ, Orzechowski R, Annis D, Honda Y. Variability of integrin alpha 2 beta 1 activity on human platelets. *Blood*. 1993;82(9):2693-703.
51. Kunicki TJ, Kritzik M, Annis DS, Nugent DJ. Hereditary variation in platelet integrin alpha 2 beta 1 density is associated with two silent polymorphisms in the alpha 2 gene coding sequence. *Blood*. 1997;89(6):1939-43.
52. Moshfegh K, Wuillemin WA, Redondo M, Lammle B, Beer JH, Liechti-Gallati S, et al. Association of two silent polymorphisms of platelet glycoprotein Ia/IIa receptor with risk of myocardial infarction: a case-control study. *Lancet*. 1999;353(9150):351-4.
53. Carlsson LE, Santoso S, Spitzer C, Kessler C, Greinacher A. The alpha2 gene coding sequence T807/A873 of the platelet collagen receptor integrin alpha2beta1 might be a genetic risk factor for the development of stroke in younger patients. *Blood*. 1999;93(11):3583-6.
54. Ye Z, Liu EH, Higgins JP, Keavney BD, Lowe GD, Collins R, et al. Seven haemostatic gene polymorphisms in coronary disease: meta-analysis of 66,155 cases and 91,307 controls. *Lancet*. 2006;367(9511):651-8.
55. Nikolopoulos GK, Tsantes AE, Bagos PG, Travlou A, Vaiopoulos G. Integrin, alpha 2 gene C807T polymorphism and risk of ischemic stroke: a meta-analysis. *Thromb Res*. 2007;119(4):501-10.
56. von Beckerath N, Koch W, Mehilli J, Bottiger C, Schomig A, Kastrati A. Glycoprotein Ia gene C807T polymorphism and risk for major adverse cardiac events within the first 30 days after coronary artery stenting. *Blood*. 2000;95(11):3297-301.
57. Potocnik AJ. Role of beta 1 integrin for hemato-lymphopoiesis in mouse development. *Curr Top Microbiol Immunol*. 2000;251:43-50.
58. Kuhn R, Schwenk F, Aguet M, Rajewsky K. Inducible gene targeting in mice. *Science*. 1995;269(5229):1427-9.
59. Matsumoto M, Seya T. TLR3: interferon induction by double-stranded RNA including poly(I:C). *Adv Drug Deliv Rev*. 2008;60(7):805-12.
60. Piwko-Czuchra A, Koegel H, Meyer H, Bauer M, Werner S, Brakebusch C, et al. Beta1 integrin-mediated adhesion signalling is essential for epidermal progenitor cell expansion. *PLoS One*. 2009;4(5):e5488. PMID: 2676508.
61. Massberg S, Gawaz M, Gruner S, Schulte V, Konrad I, Zohlnhofer D, et al. A crucial role of glycoprotein VI for platelet recruitment to the injured arterial wall in vivo. *J Exp Med*. 2003;197(1):41-9. PMID: 2193801.
62. Nieswandt B, Watson SP. Platelet-collagen interaction: is GPVI the central receptor? *Blood*. 2003;102(2):449-61.
63. Lenter M, Uhlig H, Hamann A, Jenö P, Imhof B, Vestweber D. A monoclonal antibody against an activation epitope on mouse integrin chain beta 1 blocks adhesion of

- lymphocytes to the endothelial integrin alpha 6 beta 1. *Proc Natl Acad Sci U S A*. 1993;90(19):9051-5. PMID: 47499.
64. Bazzoni G, Shih DT, Buck CA, Hemler ME. Monoclonal antibody 9EG7 defines a novel beta 1 integrin epitope induced by soluble ligand and manganese, but inhibited by calcium. *J Biol Chem*. 1995;270(43):25570-7.
 65. Harburger DS, Calderwood DA. Integrin signalling at a glance. *J Cell Sci*. 2009;122(Pt 2):159-63. PMID: 2714413.
 66. Jirouskova M, Jaiswal JK, Collier BS. Ligand density dramatically affects integrin alpha IIb beta 3-mediated platelet signaling and spreading. *Blood*. 2007;109(12):5260-9. PMID: 1890822.
 67. Farndale RW, Lisman T, Bihan D, Hamaia S, Smerling CS, Pugh N, et al. Cell-collagen interactions: the use of peptide Toolkits to investigate collagen-receptor interactions. *Biochem Soc Trans*. 2008;36(Pt 2):241-50.
 68. Moroi M, Jung SM. Platelet glycoprotein VI: its structure and function. *Thromb Res*. 2004;114(4):221-33.
 69. Lipfert L, Haimovich B, Schaller MD, Cobb BS, Parsons JT, Brugge JS. Integrin-dependent phosphorylation and activation of the protein tyrosine kinase pp125FAK in platelets. *J Cell Biol*. 1992;119(4):905-12. PMID: 2289696.
 70. Hitchcock IS, Fox NE, Prevost N, Sear K, Shattil SJ, Kaushansky K. Roles of focal adhesion kinase (FAK) in megakaryopoiesis and platelet function: studies using a megakaryocyte lineage specific FAK knockout. *Blood*. 2008;111(2):596-604. PMID: 2200856.
 71. Schaller MD. Cellular functions of FAK kinases: insight into molecular mechanisms and novel functions. *J Cell Sci*. 2010;123(Pt 7):1007-13.
 72. Schneider A, Zhang Y, Guan Y, Davis LS, Breyer MD. Differential, inducible gene targeting in renal epithelia, vascular endothelium, and viscera of Mx1Cre mice. *Am J Physiol Renal Physiol*. 2003;284(2):F411-7.
 73. Miller MW, Basra S, Kulp DW, Billings PC, Choi S, Beavers MP, et al. Small-molecule inhibitors of integrin alpha2beta1 that prevent pathological thrombus formation via an allosteric mechanism. *Proc Natl Acad Sci U S A*. 2009;106(3):719-24. PMID: 2625282.
 74. Chen J, Diacovo TG, Grenache DG, Santoro SA, Zutter MM. The alpha(2) integrin subunit-deficient mouse: a multifaceted phenotype including defects of branching morphogenesis and hemostasis. *Am J Pathol*. 2002;161(1):337-44. PMID: 1850700.
 75. Coppinger JA, O'Connor R, Wynne K, Flanagan M, Sullivan M, Maguire PB, et al. Moderation of the platelet releasate response by aspirin. *Blood*. 2007;109(11):4786-92.
 76. Shattil SJ, Haimovich B, Cunningham M, Lipfert L, Parsons JT, Ginsberg MH, et al. Tyrosine phosphorylation of pp125FAK in platelets requires coordinated signaling through integrin and agonist receptors. *J Biol Chem*. 1994;269(20):14738-45.
 77. Legate KR, Fassler R. Mechanisms that regulate adaptor binding to beta-integrin cytoplasmic tails. *J Cell Sci*. 2009;122(Pt 2):187-98.
 78. Tucker KL, Sage T, Stevens JM, Jordan PA, Jones S, Barrett NE, et al. A dual role for integrin-linked kinase in platelets: regulating integrin function and alpha-granule secretion. *Blood*. 2008;112(12):4523-31. PMID: 2597126.
 79. Kruger M, Moser M, Ussar S, Thievensen I, Luber CA, Forner F, et al. SILAC mouse for quantitative proteomics uncovers kindlin-3 as an essential factor for red blood cell function. *Cell*. 2008;134(2):353-64.
 80. Murata K, Sakon M, Kambayashi J, Yukawa M, Ariyoshi H, Shiba E, et al. The effects of okadaic acid and calyculin A on thrombin induced platelet reaction. *Biochem Int*. 1992;26(2):327-34.
 81. Takala H, Nurminen E, Nurmi SM, Aatonen M, Strandin T, Takatalo M, et al. Beta2 integrin phosphorylation on Thr758 acts as a molecular switch to regulate 14-3-3 and filamin binding. *Blood*. 2008;112(5):1853-62.
 82. van Willigen G, Hers I, Gorter G, Akkerman JW. Exposure of ligand-binding sites on platelet integrin alpha IIB/beta 3 by phosphorylation of the beta 3 subunit. *Biochem J*. 1996;314 (Pt 3):769-79. PMID: 1217123.

83. Konopatskaya O, Gilio K, Harper MT, Zhao Y, Cosemans JM, Karim ZA, et al. PKC α regulates platelet granule secretion and thrombus formation in mice. *J Clin Invest*. 2009;119(2):399-407. PMID: 2631290.
84. Ablooglu AJ, Kang J, Petrich BG, Ginsberg MH, Shattil SJ. Antithrombotic effects of targeting α IIb β 3 signaling in platelets. *Blood*. 2009;113(15):3585-92. PMID: 2668853.
85. Piersma SR, Broxterman HJ, Kapci M, de Haas RR, Hoekman K, Verheul HM, et al. Proteomics of the TRAP-induced platelet releasate. *J Proteomics*. 2009;72(1):91-109.
86. Day SM, Reeve JL, Myers DD, Fay WP. Murine thrombosis models. *Thromb Haemost*. 2004;92(3):486-94.
87. Kuijpers MJ, Pozgajova M, Cosemans JM, Munnix IC, Eckes B, Nieswandt B, et al. Role of murine integrin α 2 β 1 in thrombus stabilization and embolization: contribution of thromboxane A₂. *Thromb Haemost*. 2007;98(5):1072-80.
88. Eckly A, Hechler B, Freund M, Zerr M, Cazenave JP, Lanza F, et al. Mechanisms underlying FeCl₃-induced arterial thrombosis. *J Thromb Haemost*. 2011;9(4):779-89.
89. Holtkotter O, Nieswandt B, Smyth N, Muller W, Hafner M, Schulte V, et al. Integrin α 2-deficient mice develop normally, are fertile, but display partially defective platelet interaction with collagen. *J Biol Chem*. 2002;277(13):10789-94.
90. Rezaee F, Gijbels MJ, Offerman EH, van der Linden M, De Maat MP, Verheijen JH. Overexpression of fibrinogen in ApoE*3-Leiden transgenic mice does not influence the progression of diet-induced atherosclerosis. *Thromb Haemost*. 2002;88(2):329-34.
91. Chen H, Kahn ML. Reciprocal signaling by integrin and nonintegrin receptors during collagen activation of platelets. *Mol Cell Biol*. 2003;23(14):4764-77. PMID: 162230.
92. Gruner S, Prostredna M, Aktas B, Moers A, Schulte V, Krieg T, et al. Anti-glycoprotein VI treatment severely compromises hemostasis in mice with reduced α 2 β 1 levels or concomitant aspirin therapy. *Circulation*. 2004;110(18):2946-51.
93. Flaumenhaft R. Molecular basis of platelet granule secretion. *Arterioscler Thromb Vasc Biol*. 2003;23(7):1152-60.

Acknowledgment

I would like to thank my supervisors PD Dr. Markus Moser and Prof. Dr. Steffen Massberg for letting me work on this very interesting project and their enduring support, their stimulating ideas and their critical feedback throughout the project. Furthermore I would like to thank Prof. Dr. Reinhard Fässler for his support since the very early stages of my scientific career. I have to thank my colleagues and friends Raphael Ruppert and Pandey Dharmendra for their contribution to this work, by teaching me technical skills and helping me performing experiments. I would like to thank Verena Barocke who did the carotid ligation experiments. Finally, I would like to thank Carsten Orwat and Carolin Lenz for proofreading the manuscript.

Curriculum Vitae

Day of birth	5th of June 1981 in Lauchhammer
Profession	Assistent doctor (Cardiology) at Deutsches Herzzentrum München"
Education	1988- 2001 school education in Senftenberg June 2001 Abitur at the Gymnasium Senftenberg 10/2002- 07/2005 Medical studies at Friedrich- Schiller Universität in Jena 08/2005- 03/2007 Biomedical Science studies at University of Virginia in Charlottesville, VA,USA Master of Science in Biological and Physical Sciences. Master Thesis: Role of Focal adhesion kinase in shear signaling. (Prof. M.A. Schwartz) 04/2007- 10/2010 Medical studies at Ludwig-Maximilians-Universität Munich
Internships	06/2002 Research internship at the Robert-Koch-Institute in Berlin (Dr. E. Hild) 03/2004 Research internship at Max- Plank Institute for Biochemistry in Martinsried (Prof. R. Fässler) 02/2005 clinical elective at the Charité in Berlin (Pathology) 08/2007 clinical elective at the Max-Planck-Institute of Neurology and Psychiatry in Munich 04/2008 clinical elective at Deutsches Herzzentrum München (Internal medicine)
Scholarships	08/2005-12/2006 Fulbright-scholarship 07/2006–12/2006 American Heart Association Council sponsored student scholarship
Dissertation	03/2008–07/2011: Genetic disruption of the Kindlin-3/ β 1-integrin interaction results in defective β 1- integrin dependent platelet adhesion and granula secretion Max-Planck-Institute of Biochemistry and Deutsches Herzzentrum (PD Dr. M. Moser, Prof. Dr. R. Fässler, Prof. Dr. S. Massberg)

- Publications Focal adhesion kinase modulates activation of NF- κ B by flow in endothelial cells. Petzold T, Orr AW, Hahn C, Jhaveri K, Parsons JT, Schwartz MA; Am J Physiol Cell Physiol. 2009
- Genetic disruption of the Kindlin-3/ β 1-integrin interaction results in defective platelet adhesion and granula secretion. Tobias Petzold, , Raphael Ruppert, Dharmendra Panday, Verena Barocke, Wolfgang Siess, Reinhard Fässler, Steffen Massberg and Markus Moser (script in preparation)